CHCHD2 mutations in autosomal dominant late-onset Parkinson's disease: a genome-wide linkage and sequencing study

Manabu Funayama, Kenji Ohe, Taku Amo, Norihiko Furuya, Junji Yamaguchi, Shinji Saiki, Yuanzhe Li, Kotaro Ogaki, Maya Ando, Hiroyo Yoshino, Hiroyuki Tomiyama, Kenya Nishioka, Kazuko Hasegawa, Hidemoto Saiki, Wataru Satake, Kaoru Mogushi, Ryogen Sasaki, Yasumasa Kokubo, Shigeki Kuzuhara, Tatsushi Toda, Yoshikuni Mizuno, Yasuo Uchiyama, Kinji Ohno, Nobutaka Hattori

Lancet Neurol 2015; 14: 274–82

Published Online February 4, 2015 http://dx.doi.org/10.1016/S1474-4422(14)70266-2

See Comment page 238

Research Institute for Diseases of Old Age (M Funayama PhD, H Yoshino PhD, Prof Y Uchiyama MD, Prof N Hattori MD) and Department of Research and Therapeutics for Movement Disorders (N Furuya PhD), Graduate School of Medicine, Juntendo University, Tokyo, Japan; Division of Neurogenetics, Center for Neurological Diseases and Cancer, Nagoya University Graduate School of Medicine, Nagoya, Japan (K Ohe MD, Prof K Ohno MD); Training Program of Leaders for Integrated Medical System for Fruitful Healthy-Longevity Society (LIMS), Kyoto University Graduate School of Medicine, Kyoto, Japan (K Ohe); Department of Applied Chemistry, National Defense Academy, Yokosuka, Japan (T Amo PhD); Department of Cellular and Molecular Neuropathology[1] (J Yamaguchi MSc, Prof Y Uchiyama), Department of Neurology (M Funayama, N Furuya, S Saiki MD, Y Li MD, K Ogaki MD, M Ando MD, H Tomiyama MD, K Nishioka MD, Prof Y Mizuno MD, Prof N Hattori), and Center for Genomic and Regenerative Medicine (K Mogushi PhD), Juntendo University School of Medicine, Tokyo, Japan; Department of Neurology, National Hospital Organization, Sagamihara National Hospital, Sagamihara, Japan (K Hasegawa MD); Department of Neurology, Tazuke Kofukai Medical Research Institute and Kitano Hospital, Osaka, Japan

Summary

Background Identification of causative genes in mendelian forms of Parkinson's disease is valuable for understanding the cause of the disease. We did genetic studies in a Japanese family with autosomal dominant Parkinson's disease to identify novel causative genes.

Methods We did a genome-wide linkage analysis on eight affected and five unaffected individuals from a family with autosomal dominant Parkinson's disease (family A). Subsequently, we did exome sequencing on three patients and whole-genome sequencing on one patient in family A. Variants were validated by Sanger sequencing in samples from patients with autosomal dominant Parkinson's disease, patients with sporadic Parkinson's disease, and controls. Participants were identified from the DNA bank of the Comprehensive Genetic Study on Parkinson's Disease and Related Disorders (Juntendo University School of Medicine, Tokyo, Japan) and were classified according to clinical information obtained by neurologists. Splicing abnormalities of *CHCHD2* mutants were analysed in SH-SY5Y cells. We used the Fisher's exact test to calculate the significance of allele frequencies between patients with sporadic Parkinson's disease and unaffected controls, and we calculated odds ratios and 95% CIs of minor alleles.

Findings We identified a missense mutation (*CHCHD2*, 182C>T, Thr61Ile) in family A by next-generation sequencing. We obtained samples from a further 340 index patients with autosomal dominant Parkinson's disease, 517 patients with sporadic Parkinson's disease, and 559 controls. Three *CHCHD2* mutations in four of 341 index cases from independent families with autosomal dominant Parkinson's disease were detected by *CHCHD2* mutation screening: 182C>T (Thr61Ile), 434G>A (Arg145Gln), and 300+5G>A. Two single nucleotide variants (–9T>G and 5C>T) in *CHCHD2* were confirmed to have different frequencies between sporadic Parkinson's disease and controls, with odds ratios of 2·51 (95% CI 1·48–4·24; p=0·0004) and 4·69 (1·59–13·83, p=0·0025), respectively. One single nucleotide polymorphism (rs816411) was found in *CHCHD2* from a previously reported genome-wide association study; however, there was no significant difference in its frequency between patients with Parkinson's disease and controls in a previously reported genome-wide association study (odds ratio 1·17, 95% CI 0·96–1·19; p=0·22). In SH-SY5Y cells, the 300+5G>A mutation but not the other two mutations caused exon 2 skipping.

Interpretation *CHCHD2* mutations are associated with, and might be a cause of, autosomal dominant Parkinson's disease. Further genetic studies in other populations are needed to confirm the pathogenicity of *CHCHD2* mutations in autosomal dominant Parkinson's disease and susceptibility for sporadic Parkinson's disease, and further functional studies are needed to understand how mutant CHCHD2 might play a part in the pathophysiology of Parkinson's disease.

Funding Japan Society for the Promotion of Science; Japanese Ministry of Education, Culture, Sports, Science and Technology; Japanese Ministry of Health, Labour and Welfare; Takeda Scientific Foundation; Cell Science Research Foundation; and Nakajima Foundation.

Introduction

Parkinson's disease (MIM 168600), which is caused by the death of dopaminergic neurons in the substantia nigra, is the second most common neurodegenerative disorder. Symptoms mainly involve movement, including resting tremor, rigidity, bradykinesia, and postural instability. Most Parkinson's disease cases are sporadic; only about 11% of patients with Parkinson's disease have one or more first-degree relatives diagnosed with Parkinson's disease.[1] Nevertheless, identification of causative genes in rare familial cases can shed new light on the cause of Parkinson's disease. Most monogenic forms of neurodegenerative diseases are autosomal dominant; however, so far, only six genes have been identified for autosomal dominant forms of familial Parkinson's disease.[2–4]

Although the exact mechanisms of dopaminergic cell death are still unclear, discovery of causative genes for Parkinson's disease has enabled several processes to be proposed, such as impairments in protein degradation, oxidative stress, and mitochondrial dysfunction.[5] We aimed to identify a novel causative gene for familial

Parkinson's disease by whole-genome and exome sequencing with next-generation sequencing.

Methods

Study design and participants

Participants were selected from the DNA bank of the Comprehensive Genetic Study on Parkinson's Disease and Related Disorders (CGSPD). The CGSPD bank in the Department of Neurology at Juntendo University School of Medicine (Tokyo, Japan) collects DNA and RNA of patients with typical Parkinson's disease, patients with atypical parkinsonism, and control participants for use in case-control studies, replication studies, and the discovery of novel genetic factors for Parkinson's disease. The CGSPD DNA bank stores samples from over 3500 patients with Parkinson's disease and about 800 controls.

We selected patient and control samples according to the following criteria: participants who had a completed clinical data sheet, participants with no known pathogenic mutations for Parkinson's disease, and participants with no parental consanguinity. Patients who seemed to have an autosomal recessive mode of inheritance were excluded, as were those with a family member with Parkinson's disease but an unknown mode of inheritance. We classified patients who had affected family members in at least two consecutive generations (including the index patient) as having autosomal dominant Parkinson's disease and the remaining patients as having sporadic Parkinson's disease. All patients were diagnosed by neurologists according to the Parkinson's UK Brain Bank clinical diagnostic criteria.[6] Controls, who were hospital staff and volunteers recruited during annual medical check-ups for metabolic syndrome, were confirmed by study neurologists (RS, YK, and SK) to be free of neurological disease. All participants were classed as Japanese according to self-reported racial and ethnic data.

The study was approved by the ethics committee of Juntendo University School of Medicine and all participants gave written informed consent for inclusion in CGSPD, of which this study is a part.

Procedures

For one index patient in our DNA bank, DNA were available for patients with Parkinson's disease and unaffected family members in three generations (family A). Thus, we did linkage analysis and next-generation sequencing to identify a candidate gene in this family. We collected DNA samples from all members of family A who consented to genetic testing (eight affected and five unaffected individuals from family A; figure 1A) and confirmed that they did not have known Parkinson's disease causative gene mutations (appendix). All participants in family A were genotyped using a Genome-Wide human SNP Array 6.0 (Affymetrix, Santa Clara, CA, USA), and we did multipoint parametric linkage analyses with single nucleotide polymorphism (SNP) high throughput linkage analysis system (SNPHitLink)[7] and Merlin software.[8] We selected three patients (A-III-1, A-III-6, and A-III-17) with maximum genetic distance for exome sequencing and one patient (A-II-18) for whole-genome sequencing to complement the regions of difficulty captured by exome sequencing. We did whole-genome sequencing by 100 bp paired-end sequencing on HiSeq2000 (Illumina, San Diego, CA, USA). Sample preparation for exome sequencing was done using the SureSelect Human All Exon Kit (Agilent Technologies, Santa Clara, CA, USA), and samples were subjected to 75 bp paired-end sequencing on a GenomeAnalyzer IIx (Illumina). We did read alignment to the reference human genome (UCSC hg19) with Burrows-Wheeler Aligner version 0.5.9.[9] Single nucleotide variants (SNVs) and indels were detected in each participant by use of SAMtools version 0.1.16.[10] The variants identified by next-generation sequencing were filtered according to the following criteria: location in regions with positive log of odds greater than 1 (appendix); absence from dbSNP132; location in exons or splice sites; being carried in the heterozygous state; prediction to be non-synonymous or cause aberrant splicing; confirmation by Sanger sequencing; and not noted in our unaffected Japanese controls.

We analysed genomic sequences from index cases with autosomal dominant Parkinson's disease, patients with sporadic Parkinson's disease, and control participants by Sanger sequencing with the Applied Biosystems 3130 and 3730 Genetic Analyzer (Life Technologies, Carlsbad, CA, USA) to validate the candidate genes. Primers for Sanger sequencing were designed using ExonPrimer (appendix). The sample size needed for validation was decided on the basis of a previous genetic study that identified a causal gene for neurodegenerative disease and that included 212 controls and data from public databases for the validation of novel variants.[11] We used 1000 Genomes (1089 individuals), dbSNP138, the Human Genetic Variation Database (1208 individuals), and the National Heart, Lung, and Blood Institute (NHLBI) Exome Sequencing Project (ESP) database (6503 individuals) as public databases for the validation.

For cell culture and transfection, cells were seeded onto tissue culture plates for 5 days (SK-N-SH and SH-SY5Y cells) or 24 h (HeLa cells) before transfection. SH-SY5Y cells were used for splicing assays, SK-N-SH cells were used for localisation assays, and HeLa cells were used for splicing, localisation, and immunoelectron microscopy analyses. Cultured cells were transfected using Lipofectamine 2000 reagent (Life Technologies), according to the manufacturer's recommendations.

For splicing analysis, we cloned wild-type and mutant genomic *CHCHD2* DNA fragments (182C>T, 300+5G>A, and 434G>A) into pCR-Blunt II-TOPO vector (Life Technologies) and then transferred them to *Kpn*I-*Xho*I sites in pcDNA3.1/myc-His-A (Life Technologies), generating pcDNA3.1-CHCHD2 (wild-type, 182C>T, 300+5G>A, and 434G>A). *CHCHD2* exon 2 (wild-type

(H Saiki MD); **Division of Neurology and Molecular Brain Science, Kobe University Graduate School of Medicine, Kobe, Japan** (W Satake MD, Prof T Toda MD); **Department of Neurology, Mie University Graduate School of Medicine** (R Sasaki MD) **and Kii ALS/PDC Research Center, Mie University Graduate School of Regional Innovation Studies** (Prof Y Kokubo MD), **Tsu, Japan; and Department of Neurology and Medicine, School of Nursing, Suzuka University of Medical Science, Suzuka, Japan** (Prof S Kuzuhara MD)

Correspondence to:
Prof Nobutaka Hattori, Department of Neurology, Juntendo University School of Medicine, 2-1-1 Hongo, Bunkyo-ku, Tokyo 113-8421, Japan
nhattori@juntendo.ac.jp

For **ExonPrimer** see http://ihg.gsf.de/ihg/ExonPrimer.html

See Online for appendix

and 300+5G>A) with flanking intronic sequence (52 nucleotides upstream and 14 nucleotides downstream) was subcloned into pSPL3,[12] generating pSPL3-CHCHD2 (to analyse abberant exon 2 splicing of 300+5G>A). Total RNA was extracted 24 h after transfection using TRI Reagent (Life Technologies) followed by RQ1 DNase (Promega, Madison, WI, USA) treatment. cDNA was synthesised with random primers using Superscript II reverse transcriptase (Life Technologies) or ReverTra Ace (TOYOBO, Osaka, Japan). Two primer pairs were used for amplification to detect mutation-induced exon skipping of the transfected pcDNA splicing minigene (appendix). α-^{32}P-uridine triphosphate-labelled RNA was synthesised in the 5′ splice site of *CHCHD2* exon 2 using the Riboprobe in-vitro transcription system (Promega) with a PCR-amplified fragment, according to the manufacturer's instructions. We did an RNA-electrophoretic mobility

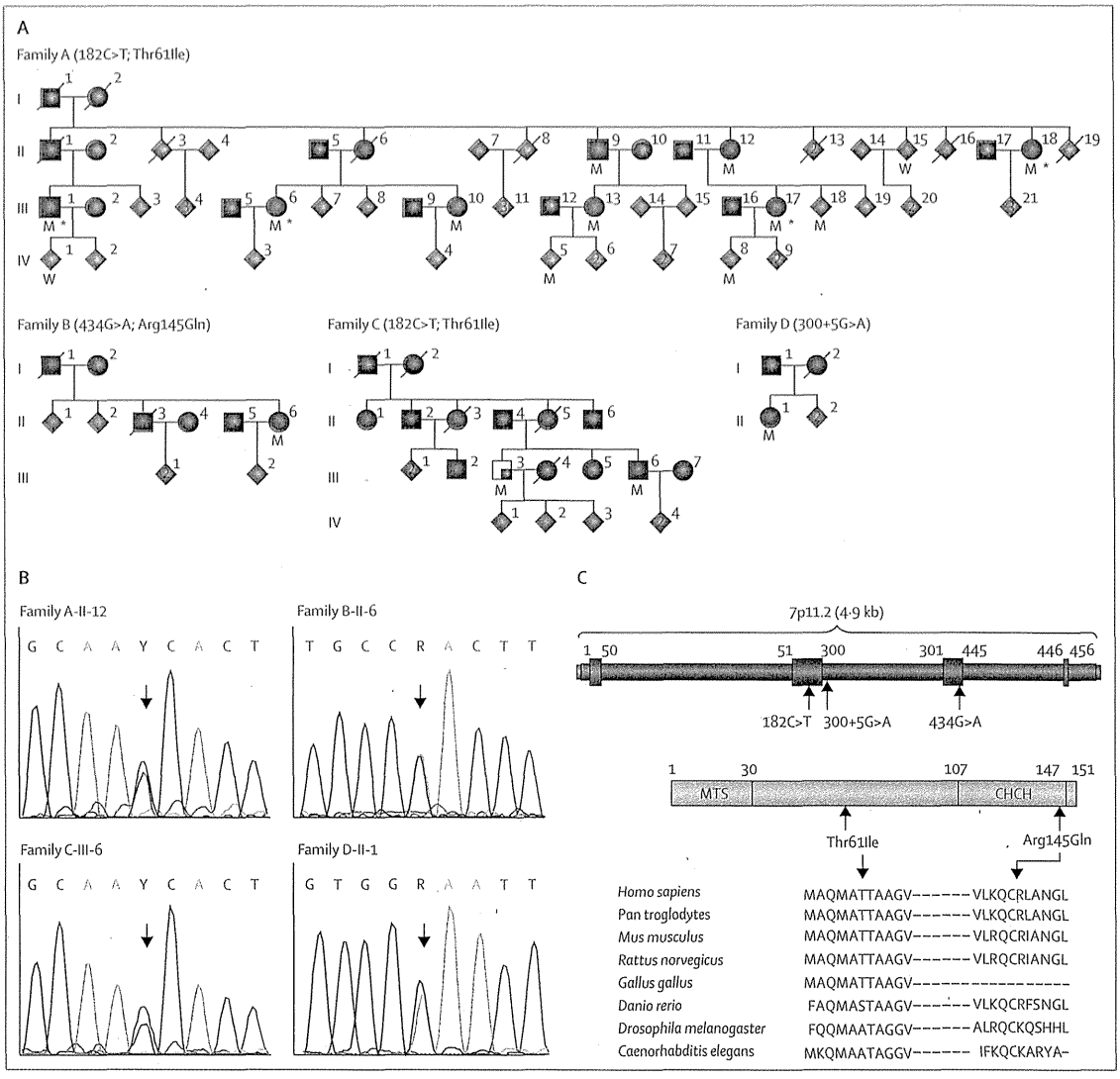

Figure 1: ***CHCHD2* mutations in four Japanese families with autosomal dominant Parkinson's disease**
(A) Pedigrees of families with *CHCHD2* mutations. M=heterozygous *CHCHD2* mutation. W=wild-type. Blue symbols represent affected individuals. Red symbols represent unaffected individuals. Numbers within red symbols represent number of unaffected offspring. The quarter-filled symbol represents an individual with essential tremor. Squares represent men. Circles represent women. Diamonds represent sex masked to protect privacy of unaffected individuals. Lines through symbols represent deceased individuals. *Participants analysed by next-generation sequencing. (B) Sequence electropherograms of identified *CHCHD2* mutations. Arrows=mutated bases. (C) Schematic representation of the *CHCHD2* locus and CHCHD2 structure. Genomic locations of identified *CHCHD2* mutations are shown in the upper part of the panel. Boxes on the line represent exons. Aminoacid locations of mutations and sequence alignment with various species are shown in the lower part. NCBI RefSeq accession numbers are as follows: *Homo sapiens*, NP_057223.1; *Pan troglodytes*, XP_003318501.1; *Mus musculus*, NP_077128.2; *Rattus norvegicus*, NP_001015019.1; *Gallus gallus*, NP_001006218.1; *Danio rerio*, NP_957061.1; *Drosophila melanogaster*, NP_573196.1; and *Caenorhabditis elegans*, NP_497826.1. CHCH=coiled-coil-helix-coiled-coil-helix domain. MTS=mitochondrial targeting sequence.

shift assay as described by Ohe and colleagues.[13] The appendix provides probe information, details of antibodies used, and supplemental methods.

Statistical analysis

SNPs with a Hardy–Weinberg equilibrium p value greater than 0·05, a minimum call rate of 1 in controls, a maximum confidence greater than 0·02, a minimum interval of 100 kb, and a minimum minor allele frequency of 0·2 were selected using SNPHitLink. We did parametric multipoint linkage analysis using Merlin software, with a disease frequency of 0·0001. The phenotypes of unaffected siblings and children of patients were described as 0 (missing phenotypes). We did case-control studies using the genotype data of ten variants that were detected in sporadic Parkinson's disease or controls, or both. We used the Fisher's exact test to calculate the significance of allele frequencies between patients with sporadic Parkinson's disease and unaffected controls. We calculated odds ratios (ORs) and 95% CIs of minor alleles found in this study using JMP 8 (SAS Institute, Drive Cary, NC, USA). In association analyses, we used the Bonferroni correction to adjust for multiple testing (ten tests), after which p values of 0·005 or lower were regarded as statistically significant, as detailed in a previous study.[14]

Role of the funding source

The funders of the study had no role in study design, data collection, data analysis, data interpretation, or writing of the report. MF and NH had full access to all the data in the study and had final responsibility for the decision to submit for publication. The other authors had access to all data except for the sequence data acquired from next-generation sequencing, to protect the privacy of personal data.

Results

The mean age at onset of the participating patients in family A (eight patients) was 55·5 years (SD 4·8; range 48–61). For validation and case-control analysis, we obtained DNA samples from 340 additional index patients with autosomal dominant Parkinson's disease, 517 patients with sporadic Parkinson's disease, and 559 controls (16 hospital staff and 543 volunteers recruited during medical check-ups; table 1).

Using next-generation sequencing, we detected a cumulative total of over 2·3 million variants in the four patients who were assessed (table 2; appendix). Our filtering criteria were satisfied by only one variant (table 2; appendix). The heterozygous 182C>T (Thr61Ile) mutation in coiled-coil-helix–coiled-coil-helix domain containing 2 (*CHCHD2*; RefSeq accession number NM_016139.2) cosegregated with Parkinson's disease in family A as assessed by Sanger sequencing of eight affected and five unaffected individuals (figure 1A and B). *CHCHD2* is located on chromosome 7p11.2 and contains four exons that encode 151 aminoacids with a predicted N-terminal mitochondrial targeting sequence (figure 1C). To validate the results of the initial genome-wide linkage analysis of family A (appendix), we did parametric multipoint linkage analysis using six microsatellites mapped to the 5′ and 3′ flanking regions of *CHCHD2*. Parametric multipoint linkage analysis by Merlin yielded a maximum log of odds score of 3·009 at D7S506 (appendix). Additionally, we did two-point linkage analysis using the 182C>T mutation as a genetic marker with a frequency of 0·0018 (1 in 560; 559 controls were sequenced in this study). As a result, the maximum log of odds score was 3·004.

To confirm whether *CHCHD2* is associated with autosomal dominant Parkinson's disease, we screened 340 index cases with autosomal dominant Parkinson's disease by Sanger sequencing and detected three additional patients with *CHCHD2* variants (families B–D; figure 1A and B). None of the three variants were noted in the 559 unaffected Japanese controls (table 3). None of the three variants detected in this study were found in 1000 Genomes, the Human Genetic Variation Database (table 3), the NHLBI ESP, or dbSNP138 (data not shown). Although the Thr61Ile variant was identified in patients from families A and C, independent founders were estimated by haplotype analysis (appendix). Altogether, we identified two missense mutations (182C>T, Thr61Ile, and 434G>A, Arg145Gln) and one splice-site mutation (300+5G>A) from four independent families with autosomal dominant Parkinson's disease.

	Number of participants	Age at onset (years)	Age at sampling (years)	Women:men ratio
Autosomal dominant Parkinson's disease	340	51·42 (13·81, 8–83)	57·99 (13·29, 17–85)	1·27
Sporadic Parkinson's disease	517	48·94 (15·11, 5–88)	57·38 (14·53, 12–92)	1·06
Controls	559	NA	58·74 (11·72, 28–89)	1·57

Data are mean (SD, range) unless otherwise specified. 340 patients were from different, independent, families, whereas family A included eight affected and five unaffected individuals; thus, family A is not included here. NA=not applicable.

Table 1: **Characteristics of participants for additional mutation screening**

	Number of variants
Total variants	2 312 760
In the linkage region	200 075
Not in db132	38 969
In exon or splice site	1018
Heterozygous	304
Predicted to be damaging*	10
Validated by Sanger sequencing	1
Not in 559 controls	1

*Predicted to be non-synonymous or cause aberrant splicing.

Table 2: **Variant filtering**

	Variant		rs number	Alternative minor allele frequency					Sporadic PD vs controls	
	cDNA	Aminoacid		Autosomal dominant PD (n=340)	Sporadic PD (n=517)	Controls (n=559)	1000 Genomes	HGVD[15]	OR (95% CI)*	p value†
chr7:56174117	-11G>A	5′UTR	rs200226056	0·000	0·000	0·00099	0·0014	ND	..	..
chr7:56174115	-9T>G	5′UTR	rs10043	0·041	0·048	0·020	0·13	0·044	2·51 (1·48–4·24)	0·0004
chr7:56174102	5C>T	Pro2Leu	rs142444896	0·035	0·018	0·004	0·008	0·013	4·69 (1·59–13·83)	0·0025
chr7:56172172	51-4A>G	Splice site	Unknown	0.000	0·00097	0·005	ND	0·004	0·19 (0·02–1·66)	0·1189
chr7:56172171	51-3C>T‡	Splice site	rs201791644	0·002	0·00097	0·000	0·00046	0·003	..	..
chr7:56172037	182C>T	Thr61Ile	Novel	0·006	0·000	0·000	ND	ND	..	..
chr7:56171964	255T>A	Ser85Arg	rs182992574	0·002	0·000	0·000	0·00092	0·002	..	..
chr7:56171914	300+5G>A	Splice site	Novel	0·002	0·000	0·000	ND	ND	..	..
chr7:56170571	434G>A	Arg145Gln	Novel	0·002	0·000	0·000	ND	ND	..	..
chr7:56169419	*125G>A	3′UTR	rs8406	0·041	0·048	0·027	0·13	ND	1·85 (1·16–2·94)	0·0112

..=not calculated because the genotypes of all of the patients with sporadic PD or controls were the major allele. HGVD=Human Genetic Variation Database.[15] ND=no data were found in database. OR=odds ratio. PD=Parkinson's disease. UTR=untranslated region. *Calculated for the minor allele. †Fisher's exact test. ‡Did not cosegregate in an autosomal dominant PD family.

Table 3: **Alternative minor allele frequencies of identified *CHCHD2* variants**

Thr61 and Arg145 are conserved residues among vertebrates (figure 1C), suggesting these sites may be of functional importance. The substitutions Thr61Ile and Arg145Gln are predicted to be pathogenic or disease causing by Polyphen2,[16] MutationTaster,[17] and SIFT.[18] Furthermore, we analysed the 300+5G>A mutation using Human Splicing Finder (version 2.4.1)[19] to predict whether it affects *CHCHD2* splicing. The 300+5G>A mutation at the 5′ splice site decreased the Human Splicing Finder score from 88·2 to 76·0, and the MaxEnt score from 6·71 to 1·62. The SD-score[20] similarly predicted that 300+5G>A causes aberrant splicing and is likely to be a splicing mutation.

To assess whether any of the mutations affect splicing in the human SH-SY5Y neuroblastoma cell line, we cloned wild-type and mutant full-length (4921 bp) genomic DNA fragments into the pcDNA3.1 mammalian expression vector. As shown in figure 2A, exon 2 splicing was not affected by pcDNA-*CHCHD2* wild-type, 182C>T, or 434G>A, but the 300+5G>A mutation caused exon 2 skipping. None of the clones affected exon 3 splicing (appendix).

We further analysed the 300+5G>A mutation in HeLa cells by inserting *CHCHD2* exon 2 and flanking introns between the two proprietary constitutive exons of a modified exon-trapping vector, pSPL3. In this heterologous context, the 300+5G>A mutation caused *CHCHD2* exon 2 exclusion (figure 2B). The exon 2-excluded mRNA generated a premature termination codon 24 nucleotides upstream of the last exon junction, and thus should be resistant to non-sense-mediated mRNA decay. The band with intermediate mobility between the exon-containing and exon-skipped bands was sequenced and shown to result from activation of an upstream cryptic-5′ splice site at position 161 in *CHCHD2* exon 2. This mRNA was predicted to be subject to non-sense-mediated mRNA decay due to a premature termination codon generated 98 nucleotides upstream of the last exon junction. We tested U1 small nuclear ribonucleoprotein (snRNP) binding to wild-type and 300+5G>A mutant 5′ splice sites with RNA electrophoresis mobility shift assays. We noted decreased U1 snRNP-binding in HeLa nuclear extracts for 300+5G>A compared with wild-type 5′ splice site RNA (figure 2C, lanes 4 and 8). We verified the mobility of the complex using purified U1 snRNP.[13] Database searches for a truncating mutation in *CHCHD2* detected a non-sense SNV, Tyr99Stop, in 1000 Genomes and dbSNP138 databases, with an allelic frequency of one in 2178. No other protein-truncating mutations were registered in the Human Genetic Variation Database or the NHLBI ESP database. This is a rare non-sense SNV and we are unable to say whether it is related to pathogenicity in Parkinson's disease or other diseases.

To investigate whether *CHCHD2* might be a susceptibility gene for sporadic Parkinson's disease, we sequenced all *CHCHD2* exons, including splice junctions, in 517 patients with sporadic Parkinson's disease and 559 controls. Two SNVs had significantly different frequencies (-9T>G, OR 2·51, 95% CI 1·48–4·24, p=0·0004; and 5C>T, 4·69, 1·59–13·83, p=0·0025; table 3). The frequencies of several variants in the control participants were slightly different to those in public databases (table 3). To confirm the link between *CHCHD2* variants and risk of sporadic Parkinson's disease, we examined a previously reported genome-wide association study on sporadic Parkinson's disease in Japanese people.[21] Although one SNP (rs816411) was found on the intron of *CHCHD2*, there was no significant difference in its frequency between patients and control participants in this genome-wide association study (OR 1·17, 95% CI 0·96–1·19, p=0·22, Cochran-Armitage trend test).[21]

CHCHD2 has a predicted N-terminal mitochondrial targeting sequence according to the UniProt database; therefore, we investigated whether CHCHD2 is located in mitochondria. Western blot analysis of subcellular fractions revealed that endogenous CHCHD2 is present in mitochondria (appendix). Furthermore, findings from confocal microscopy studies showed that exogenously expressed CHCHD2 localises to mitochondria, whereas CHCHD2 that has had the mitochondrial targeting sequence deleted does not (appendix). Immunoelectron microscopy and trypsin digestion assays showed that CHCHD2 is mainly localised in the intermembrane space (appendix). No localisation differences were noted between wild-type and missense mutants (appendix).

Table 4 summarises the clinical features of the patients with *CHCHD2* mutations. The mean age at onset of Parkinson's disease was 56·2 years (SD 8·1, range 40–67). Although a patient from family C (C-III-3; figure 1), who was examined and from whom DNA was collected after additional mutation screening with 340 index cases, mainly showed only upper limb tremor-like essential tremor, other patients presented with typical parkinsonian features, including bradykinesia, rigidity, and gait disturbance, with symptoms responsive to levodopa that are consistent with the UK Brain Bank Parkinson's disease criteria.[6] Additionally, we detected three asymptomatic carriers with heterozygous 182C>T (Thr61Ile) mutations (A-III-18, A-IV-5, and A-IV-8). Their ages at sampling were 55 years, 56 years, and 35 years, respectively.

Discussion

In this study, we show that the heterozygous 182C>T (Thr61Ile) mutation in *CHCHD2* cosegregated with Parkinson's disease in a Japanese family with autosomal dominant Parkinson's disease. We identified three *CHCHD2* variants, none of which was present in controls, and our findings suggest that *CHCHD2* is a novel gene for autosomal dominant Parkinson's disease (panel).

CHCHD2 belongs to the CHCHD protein family, which are small proteins (about <18 kDa) containing twin cysteine-x9-cysteine motifs. CHCHD proteins localise to the mitochondrial intermembrane space via the Mia40 and Erv1 disulphide relay system.[24] Proteins with the cysteine-x9-cysteine motif are involved in biogenesis and regulation of enzymes in the mitochondrial respiratory chain, from yeast to mammals.[24] In particular, CHCHD2 seems to be closely linked to cytochrome c oxidase (COX), because COX2 protein concentrations and COX activity are affected by *CHCHD2* knock down.[22,23] Moreover, CHCHD2 acts as an antiapoptotic factor in cancer cells.[25] Although further functional studies are needed to investigate how mutant CHCHD2 plays a part in Parkinson's disease in mitochondria, the combination of previously reported CHCHD2 functions and our findings suggest that mitochondrial respiration is the link to Parkinson's disease.

We identified *CHCHD2* mutations not only in patients with Parkinson's disease, but also in a patient with essential tremor from the same family. Although we do not have any dopamine transporter scan data to check for any evidence of a dopaminergic deficit, an association

For the **UniProt database** see http://www.uniprot.org

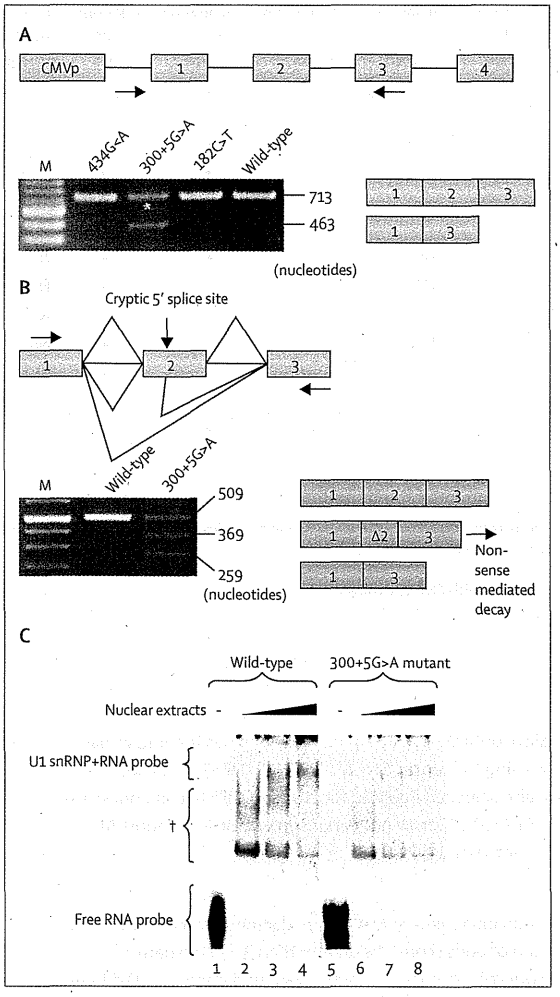

Figure 2: **Splicing assay of *CHCHD2* 300+5G>A**
(A) pcDNA-*CHCHD2*-300+5G>A induced exon 2 skipping in SH-SY5Y cells, whereas 434G>A, 182C>T, or wild-type did not. *A faint band with intermediate mobility was present between exon 2-containing and exon 2-excluded bands. (B) pSPL3-*CHCHD2*-exon 2-300+5G>A generated an exon 2-skipped transcript and a transcript with partial exon 2-inclusion via activation of an upstream cryptic 5′ splice site (arrow above exon 2). The arrows next to exons 1 and 3 show the position of primers used in the analyses. Triangles above the gene schematic denote normal splicing between exons 1 and 2, and 2 and 3, which results in a transcript with all three exons shown as a transcript bar below; the two triangles immediately below the line refer to the middle transcript bar with partial exon 2, and the lowest triangle refers to the lowest transcript bar with completely skipped exon 2. Numbers on the right side of the electrophoresis bands show their size. (C) Binding of *CHCHD2* exon 2-wild-type and 300+5G>A-mutant 5′ splice sites to U1 snRNP was measured using increasing amounts of HeLa nuclear extracts (3 μg, 6 μg, and 12 μg). Binding of the 5′ splice site probe to U1 snRNP was compromised with HeLa nuclear extracts. CMVp=cytomegalovirus promoter. M=100 bp DNA marker. snRNP=small nuclear ribonucleoprotein. †Bandshift of incomplete U1snRNP complexes.

	A-II-9	A-II-12	A-II-18	A-III-1	A-III-6	A-III-10	A-III-13	A-III-17	B-II-6	C-III-3	C-III-6	D-II-1
Sex	M	W	W	M	W	W	W	W	W	M	M	W
Age at onset (years)	60	61	55	57	59	49	55	48	67	10	40	67
Age at examination (years)	83	81	69	67	63	50	57	58	72	50	43	68
Disease duration (years)	23	20	14	10	4	1	2	10	5	40	3	1
Initial symptoms	Resting tremor	Bradykinesia	Bradykinesia	Bradykinesia	Resting tremor	Resting tremor	Bradykinesia	Resting tremor	Resting tremor	Fine tremor	Resting tremor	Gait disturbance
Hoehn and Yahr stage (on/off)	5/5	4/ND	ND/ND	3/ND	3/3	2/ND	2/ND	3/ND	3/4	ND/ND	2/ND	ND/3
Resting tremor	+	+	+	+	+	+	–	+	+	+ (fine tremor)	+	–
Bradykinesia	+	+	+	+	+	+	+	+	–	–	+	+
Rigidity	+	+	+	+	+	+	+	+	–	–	+	+
Postural instability	–	–	+	+	+	–	+	+	–	–	–	+
Asymmetry at onset	+	–	+	+	+	+	+	–	+	–	+	+
Clinical response to levodopa	+	ND	+	+	+	ND	+	+	+	ND	+	ND
Wearing off	–	ND	+	–	+	ND	–	+	–	ND	–	ND
On/off phenomenon	–	ND	–	–	–	ND	–	–	+	ND	–	ND
Levodopa-induced dyskinesia	–	ND	+	–	+	ND	–	–	–	ND	–	ND
Hyper-reflexia	–	–	–	–	+	+	–	–	+	–	–	+
Orthostatic hypotension	–	–	–	–	+	–	+	–	–	–	–	–
Constipation	–	+	+	+	+	–	+	–	–	–	–	+
Depression	–	–	–	–	–	–	–	–	–	–	–	+
Smell disturbance	–	–	–	–	–	–	–	–	–	–	–	+

All patients also had gait disturbance. No patients had urinary urgency, hallucinations, delusion, dementia, mental retardation, rapid eye movement sleep behaviour disorder, or restless legs syndrome. M=man. ND=not done. W=woman. –=not present. +=present.

Table 4: **Clinical characteristics of patients with *CHCHD2* mutations**

***Panel:* Research in context**

Systematic review

We searched PubMed, in English, until Dec 11, 2014, for known genes for autosomal dominant Parkinson's disease using the terms "SNCA", "LRRK2", "VPS35", "EIF4G1", "DCTN1" and "DNAJC13". We also searched PubMed for studies published in English using the search terms "CHCHD2", "CHCHD", "Gene AND Parkinson's disease", "import AND assembly of IMS", and "Mic17" until Dec 11, 2014.

Interpretation

We show that (1) all affected individuals in family A who had genetic tests harboured a mutation in *CHCHD2*; (2) the log of odds score was greater than 3; (3) the detected mutations were not found in our control cohort or public variant databases; (4) different mutations in the same gene were found among four families with the same disease; and (5) all detected mutations were predicted to be pathogenic by a mutations algorithm. Although this is strong evidence that *CHCHD2* mutations are associated with Parkinson's disease, only one mutation (182C>T, Thr61Ile) was confirmed to cosegregate with autosomal dominant Parkinson's disease in this study. CHCHD2 has been implicated in mitochondrial respiration and is involved in cytochrome C oxidase activity,[22,23] but no previous reports had shown that *CHCHD2* mutations are associated with disease.

between essential tremor and Parkinson's disease has been suggested by many clinical, epidemiological, neuroimaging, and genetic studies.[26] Additionally, a large family from Arkansas, USA, with Parkinson's disease, essential tremor, and restless legs syndrome has been reported.[27] *CHCHD2* mutations might be identified in this family, but to our knowledge the family has not been tested for *CHCHD2* mutations. We could not make any conclusions regarding the relation between essential tremor and *CHCHD2* mutations because only one patient with essential tremor and a *CHCHD2* mutation was detected in this study. Further studies are needed to identify whether *CHCHD2* is involved in both Parkinson's disease and essential tremor, or whether essential tremor happens to coincide with Parkinson's disease in the same family because of reduced penetrance. Recent studies have reported that *CHCHD2* expression is increased in neural stem cell lines derived from a patient with Huntington's disease (MIM 143100) and in HEK-293 cells under hypoxic conditions (4% oxygen).[22,28,29] Based on these observations, *CHCHD2* might be involved in various neurodegenerative diseases and cerebral infarction (MIM 601367).

Causative genes for mendelian forms of Parkinson's disease play an important part in mitochondrial clearance, and the clearance of damaged mitochondria is a key mechanism in the pathogenesis of Parkinson's disease and needs to be better understood. *PARK2* (MIM 602544) and *PINK1* (MIM 608309) are well known causative genes for early-onset autosomal recessive Parkinson's disease. Findings from functional studies have revealed that Parkin E3 ubiquitin ligase is fully activated by PINK1-dependent phosphorylation of both Parkin and ubiquitin on damaged mitochondria in the first phase of PINK1/parkin-mediated mitophagy.[30,31] MIX17 (YMR002W), the

yeast homolog of CHCHD2, is regulated by the ubiquitin-proteasome system.[32] Although there has been no evidence of a relation between CHCHD2 and mitophagy, whether CHCHD2 is involved in PINK1/parkin-mediated mitophagy should be investigated.

Although the Thr61Ile mutation of *CHCHD2* was confirmed in independent probands and cosegregates with Parkinson's disease, the Arg145Gln and splicing (300+5G>A) mutations were found in only one patient in a small family with autosomal dominant Parkinson's disease. Whether or not these two mutations are linked to Parkinson's disease remains unclear. We would have liked to confirm these findings by undertaking mutation screening of patients and unaffected members of families B and D, but unfortunately the patients in this study declined access to other family members. Furthermore, we could not collect RNA samples from patients with 300+5G>A mutations, which produced the splicing abnormality in SH-SY5Y cells.

Our findings differ from those from a previously reported genome-wide association study.[21] We are unsure whether our case-control study detected false positive results because of the small sample size or whether the genome-wide association study could not detect positive variants for Parkinson's disease risk because of the low allele frequencies of SNVs mapped on the *CHCHD2* region.

Contributors

MF, YM, KOhn, and NH were responsible for the concept and design of the study. MF, SS, and KOhe wrote the first draft of the paper. MF, KOhe, TA, NF, JY, SS, HY, WS, KM, KOhn, and NH revised the manuscript. MF, KOhe, TA, NF, JY, SS, YL, KOg, MA, HY, HT, KN, KH, HS, WS, KM, TT, YM, YU, KOhn, and NH acquired, analysed, and interpreted data. RS, YK, and SK collected and characterised control samples. All authors read and commented on drafts of the manuscript before submission.

Declaration of interests

MF and NH have a patent pending relating to this work. YM has received personal fees from FP Pharmaceutical, Otsuka Pharmaceutical, Abbvie, and Kyowa Hakko-Kirin. NH has received personal fees from Hisamitsu Pharmaceutical, Otsuka Pharmaceutical, Novartis Pharma, GlaxoSmithKline, Nippon Boehringer Ingelheim, FP Pharmaceutical, Dai-Nippon Sumitomo Pharma, Eisai, Kissei Pharmaceutical, Janssen Pharmaceutical, Nihon Medi-physics, Astellas Pharma, and Kyowa Hakko-Kirin. All other authors declare no competing interests.

Acknowledgments

We thank Yoko Imamichi for her assistance. We received a Grant-in-Aid for Scientific Research on Innovative Areas (25129707 to MF, 25111007 to SS, 25110720 to WS, 22129006 to TT, 23111004 to YU, 25118508 to KOhn, and 23111003 to NH), and a Grant-in-Aid for the Program for the Strategic Research Foundation at Private Universities from the Japanese Ministry of Education, Culture, Sports, Science and Technology; a Grant-in-Aid for Young Scientists (24790903 to TA, 25860725 to YL, 23689046 to SS, 25860726 to KN, 25713015 to WS, and, 26870175 to KM); a Grant-in-Aid for Challenging Exploratory Research (24659435 to SS, 25670420 to WS, 25670099 to YU and 25670164 to KOhn); a Grant-in-Aid for Scientific Research from the Japan Society for the Promotion of Science (25461291 to MF, 24591920 to KOhe, 24500868 to NF, 25305030 to YK, 24390221 to KOhn, and 24390224 to NH); a Grant-in-Aid for Health Labour Sciences Research Grant (H24-Nanchitou-Nan-Ippan-058 to YK, H26-Nanchitou-Nan-Ippan-085 to YK, TT, and NH; H23-Jitsuyouka-Nanbyou-Ippan-015 to TT; H26-Itaku-Nan-Ippan-037 to TT and NH; and H26-Itaku-Nan-Ippan-024 to KOhn) from the Japanese Ministry of Health, Labour and Welfare; and grants from the Life Science Foundation, the Takeda Scientific Foundation, the Cell Science Research Foundation, and the Nakajima Foundation (SS).

References

1 Shino MY, McGuire V, Van Den Eeden SK, et al. Familial aggregation of Parkinson's disease in a multiethnic community-based case-control study. *Mov Disord* 2010; **25:** 2587–94.
2 Singleton AB, Farrer MJ, Bonifati V. The genetics of Parkinson's disease: progress and therapeutic implications. *Mov Disord* 2013; **28:** 14–23.
3 Lautier C, Goldwurm S, Dürr A, et al. Mutations in the GIGYF2 (TNRC15) gene at the PARK11 locus in familial Parkinson disease. *Am J Hum Genet* 2008; **82:** 822–33.
4 Vilariño-Güell C, Rajput A, Milnerwood AJ, et al. DNAJC13 mutations in Parkinson disease. *Hum Mol Genet* 2014; **23:** 1794–801.
5 Schapira AH, Olanow CW, Greenamyre JT, Bezard E. Slowing of neurodegeneration in Parkinson's disease and Huntington's disease: future therapeutic perspectives. *Lancet* 2014; **384:** 545–55.
6 Hughes AJ, Daniel SE, Kilford L, Lees AJ. Accuracy of clinical diagnosis of idiopathic Parkinson's disease: a clinico-pathological study of 100 cases. *J Neurol Neurosurg Psychiatry* 1992; **55:** 181–84.
7 Fukuda Y, Nakahara Y, Date H, et al. SNP HiTLink: a high-throughput linkage analysis system employing dense SNP data. *BMC Bioinformatics* 2009; **10:** 121.
8 Abecasis GR, Cherny SS, Cookson WO, Cardon LR. Merlin—rapid analysis of dense genetic maps using sparse gene flow trees. *Nat Genet* 2002; **30:** 97–101.
9 Li H, Durbin R. Fast and accurate short read alignment with Burrows-Wheeler transform. *Bioinformatics* 2009; **25:** 1754–60.
10 Li H, Handsaker B, Wysoker A, et al. The Sequence Alignment/Map format and SAMtools. *Bioinformatics* 2009; **25:** 2078–79.
11 Saitsu H, Nishimura T, Muramatsu K, et al. De novo mutations in the autophagy gene *WDR45* cause static encephalopathy of childhood with neurodegeneration in adulthood. *Nat Genet* 2013; **45:** 445–49.
12 Masuda A, Shen XM, Ito M, Matsuura T, Engel AG, Ohno K. hnRNP H enhances skipping of a nonfunctional exon P3A in CHRNA1 and a mutation disrupting its binding causes congenital myasthenic syndrome. *Hum Mol Genet* 2008; **17:** 4022–35.
13 Ohe K, Mayeda A. HMGA1a trapping of U1 snRNP at an authentic 5′ splice site induces aberrant exon skipping in sporadic Alzheimer's disease. *Mol Cell Biol* 2010; **30:** 2220–28.
14 Sham PC, Purcell SM. Statistical power and significance testing in large-scale genetic studies. *Nat Rev Genet* 2014; **15:** 335–46.
15 Narahara M, Higasa K, Nakamura S, et al. Large-scale east-Asian eQTL mapping reveals novel candidate genes for LD mapping and the genomic landscape of transcriptional effects of sequence variants. *PLoS One* 2014; **9:** e100924.
16 Adzhubei IA, Schmidt S, Peshkin L, et al. A method and server for predicting damaging missense mutations. *Nat Methods* 2010; **7:** 248–49.
17 Schwarz JM, Rödelsperger C, Schuelke M, Seelow D. MutationTaster evaluates disease-causing potential of sequence alterations. *Nat Methods* 2010; **7:** 575–76.
18 Kumar P, Henikoff S, Ng PC. Predicting the effects of coding non-synonymous variants on protein function using the SIFT algorithm. *Nat Protoc* 2009; **4:** 1073–81.
19 Desmet, FO, Hamroun D, Lalande M, Collod-Beroud G, Claustres M, Beroud C. Human Splicing Finder: an online bioinformatics tool to predict splicing signals. *Nucleic Acid Res* 2009; **37:** e67.
20 Sahashi K, Masuda A, Matsuura T, et al. In vitro and in silico analysis reveals an efficient algorithm to predict the splicing consequences of mutations at the 5′ splice sites. *Nucleic Acids Res* 2007; **35:** 5995–6003.
21 Satake W, Nakabayashi Y, Mizuta I, et al. Genome-wide association study identifies common variants at four loci as genetic risk factors for Parkinson's disease. *Nat Genet* 2009; **41:** 1303–07.
22 Aras S, Bai M, Lee I, Springett R, Hüttemann M, Grossman LI. MNRR1 (formerly CHCHD2) is a bi-organellar regulator of mitochondrial metabolism. *Mitochondrion* 2015 **20:** 43–51.

23 Baughman JM, Nilsson R, Gohil VM, Arlow DH, Gauhar Z, Mootha VK. A computational screen for regulators of oxidative phosphorylation implicates SLIRP in mitochondrial RNA homeostasis. *PLoS Genet* 2009; **5**: e1000590.

24 Longen S, Bien M, Bihlmaier K, et al. Systematic analysis of the twin cx(9)c protein family. *J Mol Biol* 2009; **393**: 356–68.

25 Liu Y, Clegg HV, Leslie PL, et al. CHCHD2 inhibits apoptosis by interacting with Bcl-x L to regulate Bax activation. *Cell Death Differ* 2014; published online Dec 5. DOI:10.1038/cdd.2014.194.

26 Fekete R, Jankovic J. Revisiting the relationship between essential tremor and Parkinson's disease. *Mov Disord* 2011; **26**: 391–98.

27 Puschmann A, Pfeiffer RF, Stoessl AJ, et al. A family with parkinsonism, essential tremor, restless legs syndrome, and depression. *Neurology* 2011; **76**: 1623–30.

28 Feyeux M, Bourgois-Rocha F, Redfern A, et al. Early transcriptional changes linked to naturally occurring Huntington's disease mutations in neural derivatives of human embryonic stem cells. *Hum Mol Genet* 2012; **21**: 3883–95.

29 Aras S, Pak O, Sommer N, et al. Oxygen-dependent expression of cytochrome c oxidase subunit 4-2 gene.expression is mediated by transcription factors RBPJ, CXXC5 and CHCHD2. *Nucleic Acids Res* 2013; **41**: 2255–66.

30 Kondapalli C, Kazlauskaite A, Zhang N, et al. PINK1 is activated by mitochondrial membrane potential depolarization and stimulates Parkin E3 ligase activity by phosphorylating Serine 65. *Open Biol* 2012; **2**: 120080.

31 Koyano F, Okatsu K, Kosako H, et al. Ubiquitin is phosphorylated by PINK1 to activate parkin. *Nature* 2014; **510**: 162–66.

32 Bragoszewski P, Gornicka A, Sztolsztener ME, Chacinska A. The ubiquitin-proteasome system regulates mitochondrial intermembrane space proteins. *Mol Cell Biol* 2013; **33**: 2136–48.

Neuroscience Letters 580 (2014) 37–40

Contents lists available at ScienceDirect

Neuroscience Letters

journal homepage: www.elsevier.com/locate/neulet

Detailed analysis of mitochondrial respiratory chain defects caused by loss of PINK1

Taku Amo[a,*], Shinji Saiki[b], Tadashi Sawayama[a], Shigeto Sato[b], Nobutaka Hattori[b]

[a] Department of Applied Chemistry, National Defense Academy, 1-10-20 Hashirimizu, Yokosuka 239-8686, Japan
[b] Department of Neurology, Juntendo University School of Medicine, 2-1-1 Hongo, Bunkyo-ku, Tokyo 113-8421, Japan

HIGHLIGHTS

- Complete *PINK1* ablation causes mitochondrial dysfunction.
- Both complex I and complex III are defective in PINK1-deficient cells.
- Mitochondrial respiratory chain defects may be associated with PD pathogenesis.

ARTICLE INFO

Article history:
Received 6 May 2014
Received in revised form 10 July 2014
Accepted 25 July 2014
Available online 1 August 2014

Keywords:
Parkinson's disease
Mitochondria
PINK1
Respiratory chain

ABSTRACT

Mutations in *PTEN-induced putative kinase 1* (*PINK1*) cause recessive forms of Parkinson's disease (PD). PINK1 acts upstream of parkin, regulating mitochondrial elimination (mitophagy) in cultured cells treated with mitochondrial uncouplers that cause mitochondrial depolarization. PINK1 loss-of-function decreases mitochondrial membrane potential, resulting in mitochondrial dysfunction, although the exact function of PINK1 in mitochondria has not been fully elucidated. We have previously found that PINK1 deficiency causes a decrease in mitochondrial membrane potential, which is not due to a proton leak, but to respiratory chain defects. Here, we examine mitochondrial respiratory chain defects in PINK1-deficient cells, and find both complex I and complex III are defective. These results suggest that mitochondrial respiratory chain defects may be associated with PD pathogenesis caused by mutations in the *PINK1* gene.

1. Introduction

Parkinson's disease (PD) is a neurodegenerative disease characterized by loss of dopaminergic neurons in the substantia nigra. Mitochondrial dysfunction has been proposed as a major factor in sporadic and familial PD pathogenesis [1]. In the early 1980s, it was discovered that a neurotoxin, 1-methyl-4-phenyl-1,2,3,6-tetrahydropyridine (MPTP), could inhibit mitochondrial complex I and cause parkinsonian symptoms in humans [17,20]. MPTP and other complex I inhibitors (e.g., rotenone), reproduce clinical features of PD in animals and are commonly used to model PD [5]. Moreover, complex I deficiency is frequently observed in the substantia nigra of PD patients at autopsy [12].

Mutations in the *parkin*, *PINK1* (PTEN-induced putative kinase 1), and *DJ-1* genes lead to autosomal recessive parkinsonism [1]. Although these gene products have not been fully characterized, they are strongly implicated in mitochondrial homeostasis [9]. PINK1 contains an N-terminal mitochondrial targeting sequence and a serine/threonine kinase domain [28]. Loss of PINK1 function induces increased vulnerability to various stresses [10,27]. Because parkin can rescue PINK1 deficiency, but not vice versa, PINK1 must act upstream of parkin in the same genetic pathway [8,25]. PINK1 loss-of-function decreases mitochondrial membrane potential [7] and the PINK1-parkin pathway is associated with mitochondrial autophagy (mitophagy) in cultured cells treated with the mitochondrial uncoupler, carbonyl cyanide *m*-chlorophenylhydrazone (CCCP), which causes mitochondrial depolarization [19,24]. However, the exact function of PINK1 in mitochondria has not been fully elucidated.

We have previously found that *PINK1* deficiency in cultured cells causes a decrease in mitochondrial membrane potential that is not due to a proton leak, but to respiratory chain defects [3]. Similar respiration defects are observed in *PINK1* knock-out mice [10] and

Abbreviations: BN-PAGE, blue native PAGE; CCCP, carbonyl cyanide *m*-chlorophenylhydrazone; mtDNA, mitochondrial DNA; MEFs, mouse embryonic fibroblasts; MPTP, 1-methyl-4-phenyl-1,2,3,6-tetrahydropyridine; PD, Parkinson's disease; PINK1, PTEN induced putative kinase 1.

* Corresponding author. Tel.: +81 46 841 3810; fax: +81 46 844 5901.
E-mail address: amo@nda.ac.jp (T. Amo).

http://dx.doi.org/10.1016/j.neulet.2014.07.045
0304-3940/

complex I deficiency is observed in *PINK1* mutant flies [22] and human fibroblasts from patients with *PINK1* mutations [13]. Interestingly, in flies, some *PINK1* mutant phenotypes are mimicked by downregulation of a complex I component and rescued by Ndi1p, a yeast NADH:ubiquinone oxidoreductase that can bypass complex I [29]. Most recently, it was reported that PINK1 is needed to maintain complex I activity via NdufA10 phosphorylation [21]. Thus, as a respiration defect is a likely key event of PINK1 deficiency, here, we provide a detailed analysis of mitochondrial respiratory chain defects in our *PINK1*-deficient cell model.

2. Materials and methods

2.1. PINK1 knock-out mouse embryonic fibroblasts (MEFs)

PINK1 knock-out MEFs were prepared and cultured as previously described [3,19]. Mitochondria were prepared from cultured MEFs as previously described [2].

2.2. Quantitative polymerase chain reaction (PCR) to estimate mitochondrial DNA copy number

Total DNA was prepared from cultured cells by incubating in a solution of 75 mM NaCl, 50 mM EDTA, 0.5% SDS, and 0.5 mg/mL proteinase K at 50 °C for 2 h. DNA was precipitated by adding of an equal volume of isopropanol, then pelleted by centrifugation, and dissolved in TE buffer. Mitochondrial DNA copy number was estimated by quantitative real-time PCR assays using the MyiQ2 Real Time PCR Detection System (Bio-Rad). The sequences of primers and probes were as follows: cytochrome *c* oxidase I gene (COX1, mitochondrial DNA): forward primer 5′-TGATTCCCATTATTTTCAGGCTTC-3′, reverse primer 5′-ACTCCTACGAATATGATGGCGAA-3′, probe 5′-CCCTAGATGACACATGAGCAAAAGCCCA-3′; glyceraldehyde 3-phosphate dehydrogenase gene (GAPDH, nuclear DNA): forward primer 5′-CATCACTGCCACCCAGAAGA-3′, reverse primer 5′-ATGTTCTGGGCAGCCCC-3′, probe 5′-TGGATGGCCCCTCTGGAAAGCTG-3′.

2.3. Respiratory chain enzyme assays

Individual enzyme activities of complexes I, II, III, and IV were measured at 30 °C as previously described [4]. Complex I activity was measured by monitoring NADH oxidation at 340 nm (minus background of 425 nm). Rotenone (2 μg/mL) was used to confirm complex I-specific activity. Complex II activity was measured by monitoring 2,6-dichlorophenolindophenol reduction of at 600 nm. Complexes III and IV activities were measured by monitoring reduction or oxidation, respectively, of cytochrome *c* at 550 nm (minus background of 580 nm). Citrate synthase was assayed by monitoring 5,5′-dithiobis(2-nitrobenzoic acid) reduction at 412 nm, as previously described [15].

2.4. Blue native PAGE (BN-PAGE)

BN-PAGE was performed as previously described [30]. Mitochondria prepared from MEFs were solubilized with 1% *n*-dodecyl-β-D-maltoside or 1% digitonin and centrifuged at 20,000 × *g* for 10 min at 4 °C. Supernatants with Coomassie brilliant blue G-250 added (0.2% final concentration), were electrophoresed through 5–13% polyacrylamide gradient gels and were subjected to immunoblotting. Densitometry analysis was performed using ImageJ (NIH).

2.5. Antibodies

Antibodies used in this study as follows: anti-actin (clone C4, Millipore), anti-complex I subunit NDUFA9 (MS111, Mitosciences), anti-complex II subunit 70 kDa Fp (M204, Mitosciences), anti-complex III subunit Core I (MS303, Mitosciences), anti-complex IV subunit IV (MS408, Mitosciences), anti-ATP synthase subunit β (a gift from Dr. Ueno at Juntendo University, Tokyo, Japan), anti-VDAC (MSA03, Mitosciences), and anti-TFAM (a gift from Dr. Kang at Kyushu University, Fukuoka, Japan).

2.6. Statistics

Values are presented as means ± SEM (standard error of the mean). The significance of differences between means was assessed

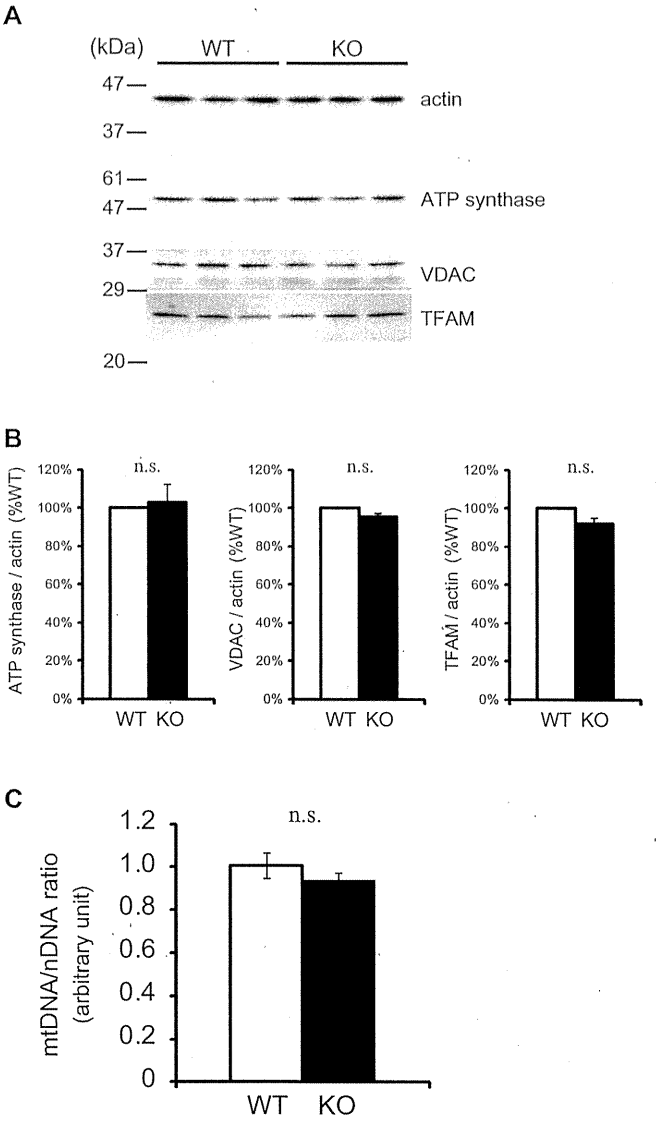

Fig. 1. Mitochondrial protein contents and mtDNA contents of *PINK1*$^{+/+}$ and $^{-/-}$ MEFs. (A) Representative images of mitochondrial marker proteins analyzed by immunoblotting after SDS-PAGE. (B) Densitometry analysis of mitochondrial proteins to actin ratio was performed using three independent experiments. (C) Mitochondrial DNA copy number of *PINK1*$^{+/+}$ and $^{-/-}$ MEFs. Open bars, *PINK1*$^{+/+}$ MEFs; closed bars, *PINK1*$^{-/-}$ MEFs. Error bars indicate SEM ($n = 3$). n.s., not significant.

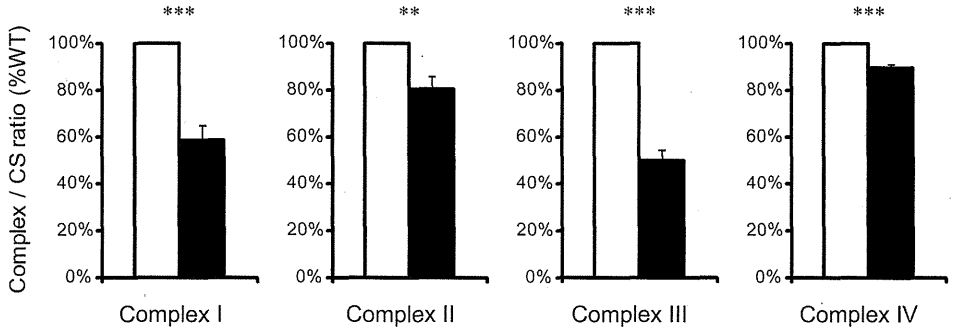

Fig. 2. Respiratory chain complex activities in mitochondria isolated from *PINK1*$^{+/+}$ and $^{-/-}$ MEFs. Open bars, *PINK1*$^{+/+}$ MEFs; closed bars, *PINK1*$^{-/-}$ MEFs. Each complex activity was normalized to citrate synthase activity measured in the same samples. Data are expressed as percentages of levels in *PINK1*$^{+/+}$ cells (%WT). Error bars indicate SEM ($n = 4$ independent mitochondrial preparations). $^{*}P < 0.05$; $^{**}P < 0.01$; $^{***}P < 0.001$.

by the unpaired Student's *t*-test; *P* values < 0.05 were taken to be significant.

3. Results and discussion

3.1. Mitochondrial content

To estimate mitochondrial content in *PINK1*$^{+/+}$ and $^{-/-}$ MEFs, we determined the expression levels of mitochondrial proteins, VDAC (porin) and ATP synthase (complex V). These two proteins are known as relatively stable mitochondrial proteins and often used as SDS-PAGE loading control of isolated mitochondria. Furthermore, we have previously reported that mitochondrial phosphorylating system including ATP synthase was not functionally altered by loss of PINK1 [3]. As shown in Fig. 1A and B, the mitochondrial proteins were not different between *PINK1*$^{+/+}$ and $^{-/-}$ MEFs. We also determined the mitochondrial DNA (mtDNA) copy number. While the mtDNA copy number does not strictly correlate with mitochondrial content, it is usually a good indicator and its determination is rapid and less labor intensive. Mitochondrial DNA copy numbers were similar in *PINK1*$^{+/+}$ and $^{-/-}$ MEFs (Fig. 1C). Mitochondrial transcriptional factor A (TFAM), which binds mtDNA in a sequence-independent manner and their contents finely correlated with mtDNA copy number [14], was also same expression level (Fig. 1A). Therefore, the mitochondrial respiration defect in *PINK1*$^{-/-}$ MEFs is not due to a reduction in mitochondrial content.

Similar to *PINK1*$^{-/-}$ MEFs in this study, fibroblasts from a patient homozygous for the W437X missense mutation of *PINK1*, showed no changes in the mtDNA copy number [26]. Additionally, mitochondrial content was not altered in the striatum of *PINK1*$^{-/-}$ mice [10], consistent with the results of our study. However, PINK1 dysfunction causes a decreased mtDNA copy number in human SH-SY5Y neuroblastoma cells [11]. This discrepancy might be due to the type of cells. In fact, mtDNA contents of both of the MEFs (Fig. 1C) and the patient fibroblasts [26] were not significantly different from their controls, but showed slightly decreasing tendency.

3.2. Enzymatic activity of each respiratory chain complex

Previously, we found decreased mitochondrial membrane potential caused by loss of PINK1, the key event for subsequent mitochondrial elimination, was not due to a proton leak, but to respiratory chain defects [3]. To further investigate this, we determined the enzymatic activities of each respiratory chain complex.

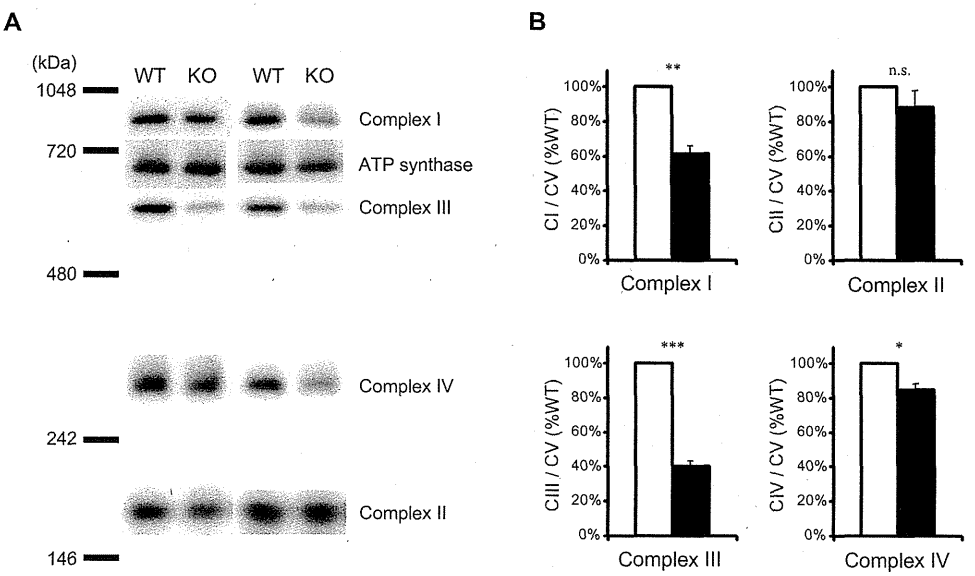

Fig. 3. Respiratory chain complex quantities in mitochondria isolated from *PINK1*$^{+/+}$ and $^{-/-}$ MEFs. (A) Representative images of respiratory chain complexes analyzed by immunoblotting after BN-PAGE. (B) Densitometry analysis of respiratory chain complexes to ATP synthase ratio was performed using three independent mitochondrial preparations. Open bars, *PINK1*$^{+/+}$ MEFs; closed bars, *PINK1*$^{-/-}$ MEFs. Error bars indicate SEM ($n = 3$). n.s., not significant; $^{*}P < 0.05$; $^{**}P < 0.01$; $^{***}P < 0.001$.

Enzymatic activities of all four respiratory chain complexes were decreased by loss of PINK1 (Fig. 2), with a dramatic reduction in complexes I and III activities in *PINK1*$^{-/-}$ MEFs.

3.2.1. Protein quantity of each respiratory chain complex

Decreased enzymatic activities per mitochondrial protein (Fig. 2) may be due to a decreased respiratory chain complex content per mitochondrial protein, or decreased enzymatic activities of each complex, or both. To assess these possibilities, we separated respiratory chain complexes in enzymatically active forms using BN-PAGE [30], and then detected each complex by immunoblotting (Fig. 3). Protein contents of all four respiratory chain complexes were decreased by loss of PINK1. In particular, complexes I and III contents were dramatically reduced in *PINK1*$^{-/-}$ MEFs. As the respiratory complex contents are in good agreement with their enzymatic activities, it is conceivable that decreased enzymatic activities per mitochondrial protein are not due to decreased enzymatic activities of each complex, but to decreased respiratory chain complex content per mitochondrial protein.

As complex I inhibitors such as MPTP and rotenone can cause parkinsonian symptoms in human and animal models, complex I defects are thought to be one of the main factors of PD pathogenesis [5,17,20]. According to recent reports, PINK1 is needed to maintain complex I activity through NdufA10 phosphorylation [21] and PINK1 deficiency can be rescued by Ndi1p, a yeast NADH:ubiquinone oxidoreductase that can bypass complex I [29]. In this study, we show that not only complex I but also complex III are deficient in *PINK1*$^{-/-}$ MEFs. Combined complexes I and III deficiencies were previously reported in patients harboring mutations in the *NDUFS4* gene of complex I [6], or the *MT-CYB* gene of complex III [16]. These are presumably due to respiratory chain supercomplexes, large assemblies of respiratory chain complexes with small electron carriers for stabilization and enhancement of electron transport [18,23]. Studies on the supercomplex status of *PINK1*$^{-/-}$ MEFs are under way.

Acknowledgements

This work was supported by Grant-in-Aid for Young Scientists (T.A.) and for Challenging Exploratory Research (S. Saiki) from JSPS, and grants from the Kanagawa Nanbyo Study Foundation (T.A.) and the Takeda Scientific Foundation (S. Saiki). We thank Drs. Clement Gautier and Jie Shen (Harvard Medical School, Boston, MA, USA) for providing *PINK1* knock-out mice, Dr. Noriyuki Matsuda (Tokyo Metropolitan Institute of Medical Science, Tokyo, Japan) for assistance to obtain immortalized cells, Dr. Takashi Ueno (Juntendo University, Tokyo, Japan) for providing anti-ATP synthase subunit β antibody, and Dr. Dongchon Kang (Kyushu University, Fukuoka, Japan) for providing anti-TFAM antibody.

References

[1] P.M. Abou-Sleiman, M.M. Muqit, N.W. Wood, Expanding insights of mitochondrial dysfunction in Parkinson's disease, Nat. Rev. Neurosci. 7 (2006) 207–219.
[2] T. Amo, M.D. Brand, Were inefficient mitochondrial haplogroups selected during migrations of modern humans? A test using modular kinetic analysis of coupling in mitochondria from cybrid cell lines, Biochem. J. 404 (2007) 345–351.
[3] T. Amo, S. Sato, S. Saiki, A.M. Wolf, M. Toyomizu, C.A. Gautier, J. Shen, S. Ohta, N. Hattori, Mitochondrial membrane potential decrease caused by loss of PINK1 is not due to proton leak, but to respiratory chain defects, Neurobiol. Dis. 41 (2011) 111–118.
[4] M.A. Birch-Machin, D.M. Turnbull, Assaying mitochondrial respiratory complex activity in mitochondria isolated from human cells and tissues, Methods Cell Biol. 65 (2001) 97–117.
[5] J. Blesa, S. Phani, V. Jackson-Lewis, S. Przedborski, Classic and new animal models of Parkinson's disease, J. Biomed. Biotechnol. 2012 (2012) 845618.
[6] S.M. Budde, L.P. van den Heuvel, A.J. Janssen, R.J. Smeets, C.A. Buskens, L. DeMeirleir, R. Van Coster, M. Baethmann, T. Voit, J.M. Trijbels, J.A. Smeitink, Combined enzymatic complex I and III deficiency associated with mutations in the nuclear encoded NDUFS4 gene, Biochem. Biophys. Res. Commun. 275 (2000) 63–68.
[7] C.T. Chu, P.I.N.K1. Tickled, Mitochondrial homeostasis and autophagy in recessive Parkinsonism, Biochim. Biophys. Acta 1802 (2010) 20–28.
[8] I.E. Clark, M.W. Dodson, C. Jiang, J.H. Cao, J.R. Huh, J.H. Seol, S.J. Yoo, B.A. Hay, M. Guo, Drosophila pink1 is required for mitochondrial function and interacts genetically with *parkin*, Nature 441 (2006) 1162–1166.
[9] N. Exner, A.K. Lutz, C. Haass, K.F. Winklhofer, Mitochondrial dysfunction in Parkinson's disease: molecular mechanisms and pathophysiological consequences, EMBO J. 31 (2012) 3038–3062.
[10] C.A. Gautier, T. Kitada, J. Shen, Loss of PINK1 causes mitochondrial functional defects and increased sensitivity to oxidative stress, Proc. Natl. Acad. Sci. U.S.A. 105 (2008) 11364–11369.
[11] M.E. Gegg, J.M. Cooper, A.H. Schapira, J.W. Taanman, Silencing of PINK1 expression affects mitochondrial DNA and oxidative phosphorylation in dopaminergic cells, PLoS ONE 4 (2009) e4756.
[12] N. Hattori, M. Tanaka, T. Ozawa, Y. Mizuno, Immunohistochemical studies on complexes I, II, III, and IV of mitochondria in Parkinson's disease, Ann. Neurol. 30 (1991) 563–571.
[13] H.H. Hoepken, S. Gispert, B. Morales, O. Wingerter, D. Del Turco, A. Mulsch, R.L. Nussbaum, K. Muller, S. Drose, U. Brandt, T. Deller, B. Wirth, A.P. Kudin, W.S. Kunz, G. Auburger, Mitochondrial dysfunction, peroxidation damage and changes in glutathione metabolism in PARK6, Neurobiol. Dis. 25 (2007) 401–411.
[14] D. Kang, S.H. Kim, N. Hamasaki, Mitochondrial transcription factor A (TFAM): roles in maintenance of mtDNA and cellular functions, Mitochondrion 7 (2007) 39–44.
[15] D.M. Kirby, D.R. Thorburn, D.M. Turnbull, R.W. Taylor, Biochemical assays of respiratory chain complex activity, Methods Cell Biol. 80 (2007) 93–119.
[16] E. Lamantea, F. Carrara, C. Mariotti, L. Morandi, V. Tiranti, M. Zeviani, A novel nonsense mutation (Q352X) in the mitochondrial cytochrome *b* gene associated with a combined deficiency of complexes I and III, Neuromuscul. Disord. 12 (2002) 49–52.
[17] J.W. Langston, P. Ballard, J.W. Tetrud, I. Irwin, Chronic Parkinsonism in humans due to a product of meperidine-analog synthesis, Science 219 (1983) 979–980.
[18] E. Lapuente-Brun, R. Moreno-Loshuertos, R. Acin-Perez, A. Latorre-Pellicer, C. Colas, E. Balsa, E. Perales-Clemente, P.M. Quiros, E. Calvo, M.A. Rodriguez-Hernandez, P. Navas, R. Cruz, A. Carracedo, C. Lopez-Otin, A. Perez-Martos, P. Fernandez-Silva, E. Fernandez-Vizarra, J.A. Enriquez, Supercomplex assembly determines electron flux in the mitochondrial electron transport chain, Science 340 (2013) 1567–1570.
[19] N. Matsuda, S. Sato, K. Shiba, K. Okatsu, K. Saisho, C.A. Gautier, Y.S. Sou, S. Saiki, S. Kawajiri, F. Sato, M. Kimura, M. Komatsu, N. Hattori, K. Tanaka, PINK1 stabilized by mitochondrial depolarization recruits Parkin to damaged mitochondria and activates latent Parkin for mitophagy, J. Cell Biol. 189 (2010) 211–221.
[20] Y. Mizuno, T. Saitoh, N. Sone, Inhibition of mitochondrial NADH-ubiquinone oxidoreductase activity by 1-methyl-4-phenylpyridinium ion, Biochem. Biophys. Res. Commun. 143 (1987) 294–299.
[21] V.A. Morais, D. Haddad, K. Craessaerts, P.J. De Bock, J. Swerts, S. Vilain, L. Aerts, L. Overbergh, A. Grunewald, P. Seibler, C. Klein, K. Gevaert, P. Verstreken, B. De Strooper, PINK1 loss of function mutations affect mitochondrial complex I activity via NdufA10 ubiquinone uncoupling, Science 344 (2014) 203–207.
[22] V.A. Morais, P. Verstreken, A. Roethig, J. Smet, A. Snellinx, M. Vanbrabant, D. Haddad, C. Frezza, W. Mandemakers, D. Vogt-Weisenhorn, R. Van Coster, W. Wurst, L. Scorrano, B. De Strooper, Parkinson's disease mutations in PINK1 result in decreased Complex I activity and deficient synaptic function, EMBO Mol. Med. 1 (2009) 99–111.
[23] D. Moreno-Lastres, F. Fontanesi, I. Garcia-Consuegra, M.A. Martin, J. Arenas, A. Barrientos, C. Ugalde, Mitochondrial complex I plays an essential role in human respirasome assembly, Cell Metabolism 15 (2012) 324–335.
[24] D. Narendra, A. Tanaka, D.F. Suen, R.J. Youle, Parkin is recruited selectively to impaired mitochondria and promotes their autophagy, J. Cell Biol. 183 (2008) 795–803.
[25] J. Park, S.B. Lee, S. Lee, Y. Kim, S. Song, S. Kim, E. Bae, J. Kim, M. Shong, J.M. Kim, J. Chung, Mitochondrial dysfunction in *Drosophila PINK1* mutants is complemented by *parkin*, Nature 441 (2006) 1157–1161.
[26] C. Piccoli, M. Ripoli, G. Quarato, R. Scrima, A. D'Aprile, D. Boffoli, M. Margaglione, C. Criscuolo, G. De Michele, A. Sardanelli, S. Papa, N. Capitanio, Coexistence of mutations in *PINK1* and mitochondrial DNA in early onset parkinsonism, J. Med. Genet. 45 (2008) 596–602.
[27] J.W. Pridgeon, J.A. Olzmann, L.S. Chin, L. Li, PINK1 protects against oxidative stress by phosphorylating mitochondrial chaperone TRAP1, PLoS Biol. 5 (2007) e172.
[28] E.M. Valente, P.M. Abou-Sleiman, V. Caputo, M.M. Muqit, K. Harvey, S. Gispert, Z. Ali, D. Del Turco, A.R. Bentivoglio, D.G. Healy, A. Albanese, R. Nussbaum, R. González-Maldonado, T. Deller, S. Salvi, P. Cortelli, W.P. Gilks, D.S. Latchman, R.J. Harvey, B. Dallapiccola, G. Auburger, N.W. Wood, Hereditary early-onset Parkinson's disease caused by mutations in *PINK1*, Science 304 (2004) 1158–1160.
[29] S. Vilain, G. Esposito, D. Haddad, O. Schaap, M.P. Dobreva, M. Vos, S. Van Meensel, V.A. Morais, B. De Strooper, P. Verstreken, The yeast complex I equivalent NADH dehydrogenase rescues *pink1* mutants, PLoS Genet. 8 (2012) e1002456.
[30] I. Wittig, H.P. Braun, H. Schägger, Blue native PAGE, Nat. Protoc. 1 (2006) 418–428.

OPEN ACCESS Freely available online

PLOS | ONE

Identification of Licopyranocoumarin and Glycyrurol from Herbal Medicines as Neuroprotective Compounds for Parkinson's Disease

Takahiro Fujimaki[1], Shinji Saiki[2], Etsu Tashiro[1], Daisuke Yamada[2], Mitsuhiro Kitagawa[1], Nobutaka Hattori[2]*, Masaya Imoto[1]*

1 Department of Biosciences and Informatics, Faculty of Science and Technology, Keio University, Yokohama, Japan, **2** Department of Neurology, Juntendo University School of Medicine, Bunkyo, Tokyo

Abstract

In the course of screening for the anti-Parkinsonian drugs from a library of traditional herbal medicines, we found that the extracts of *choi-joki-to* and *daio-kanzo-to* protected cells from MPP^+-induced cell death. Because *choi-joki-to* and *daio-kanzo-to* commonly contain the genus *Glycyrrhiza*, we isolated licopyranocoumarin (LPC) and glycyrurol (GCR) as potent neuroprotective principals from *Glycyrrhiza*. LPC and GCR markedly blocked MPP^+-induced neuronal PC12D cell death and disappearance of mitochondrial membrane potential, which were mediated by JNK. LPC and GCR inhibited MPP^+-induced JNK activation through the suppression of reactive oxygen species (ROS) generation, thereby inhibiting MPP^+-induced neuronal PC12D cell death. These results indicated that LPC and GCR derived from *choi-joki-to* and *daio-kanzo-to* would be promising drug leads for PD treatment in the future.

Citation: Fujimaki T, Saiki S, Tashiro E, Yamada D, Kitagawa M, et al. (2014) Identification of Licopyranocoumarin and Glycyrurol from Herbal Medicines as Neuroprotective Compounds for Parkinson's Disease. PLOS ONE 9(6): e100395. doi:10.1371/journal.pone.0100395

Editor: Hiroyoshi Ariga, Hokkaido University, Japan

Received March 6, 2014; **Accepted** May 19, 2014; **Published** June 24, 2014

Data Availability: The authors confirm that all data underlying the findings are fully available without restriction. All data are included within the paper and its Supporting Information files.

Funding: This work was supported by Health Labour Sciences Research Grants from the Ministry of Health, Labour and Welfare of Japan. The extract powder of 128 traditional herbal (kampo) medicines (The Kampo, TJ-1~3, TJ-5~12, TJ-14~41, TJ-43, TJ-45~48, TJ-50~93, TJ-95~128, TJ-133~138) and powder of Glycyrrhiza were kindly donated from Tsumura Corporation (Tokyo, Japan). The funders had no role in study design, data collection and analysis, decision to publish, or preparation of the manuscript.

Competing Interests: The extract powder of 128 traditional herbal (kampo) medicines (The Kampo, TJ-1~3, TJ-5~12, TJ-14~41, TJ-43, TJ-45~48, TJ-50~93, TJ-95~128, TJ-133~138) and powder of Glycyrrhiza were kindly donated from Tsumura Corporation (Tokyo, Japan). This does not alter the authors' adherence to PLOS ONE policies on sharing data and materials.

* Email: nhattori@juntendo.ac.jp (NH); imoto@bio.keio.ac.jp (MI)

Introduction

Parkinson's disease (PD) is a common neurodegenerative disease characterized by progressive dopaminergic neuronal cell death in the substantia nigra par compacta of the midbrain. The main symptoms of PD are movement disorders such as tremors, bradykinesia/akinesia, rigidity, postural instability, and gait abnormalities. Although deep-brain stimulation and oral administration of L-dopa, dopamine agonists and amantadine hydrochloride have been well established as symptomatic treatments, there are no therapies to completely cure patients with the disorder [1]. Mitochondrial dysfunction, especially dysfunction of the mitochondrial electron transport chain mainly relying on complex I activity, has been implicated in the disease's pathogenesis. In addition to defects of complex I in postmortem brains, skeletal muscle and platelets of patients with PD [2,3,4,5,6], cybrid cells containing mtDNA derived from PD platelets have indicated complex I defects [7,8,9]. Because various rodents treated with mitochondrial toxins such as rotenone, 1-methyl-4-phenyl-1,2,3,6-tetrahydropyridine (MPTP), and its toxic metabolite 1-methyl-4-phenylpyridinium (MPP^+) show motor deficits associated with selective loss of dopaminergic neurons, they have been widely used as acquired PD models [10,11,12,13,14,15]. Selegiline, a medication widely used at present, has the capacity to protect dopamine neurons by inhibiting MAO-B oxidation for conversion of MPTP into MPP^+ and blocking the formation of free radicals derived from the oxidative metabolism of dopamine [16,17]. Also, MPP^+ models offer unexploited therapeutic potential for some atypical antipsychotics (olanzapine, aripiprazole, and ziprasidone) and the anticonvulsant zonisamide in PD, and new mechanisms of neuroprotective effects of FLZ (which activates HSP27/HSP70) and paeoniflorin (which modulates autophagy) have led to treatments for PD [18,19,20,21].

Herbal medicines are employed to treat PD in ancient medical systems in Asian countries such as India, China, Japan, and Korea based on anecdotal and experience-based theories [22]. The traditional herbal medicines *yi-gan san* and *modified yeoldahanso-tang* have neuroprotective effects and can rescue dopaminergic neurons from MPP^+/MPTP toxicity using both *in vitro* and *in vivo* methods [23,24]. Several compounds derived from herbal medicines also exert anti-Parkinsonian activities. For instance, ginsenoside Rb1 isolated from *Panax ginseng C. A. Meyer*, 3-*O*-demethylswertipunicoside isolated from *S. punicea*, and salidroside isolated from *Rhodiola rosea L.*, have been reported to attenuate MPP^+-induced neurotoxicity in PC12 cells *in vitro* [25,26,27]. However, clinical evidence for the efficacy and safety of these herbal medicines for PD is

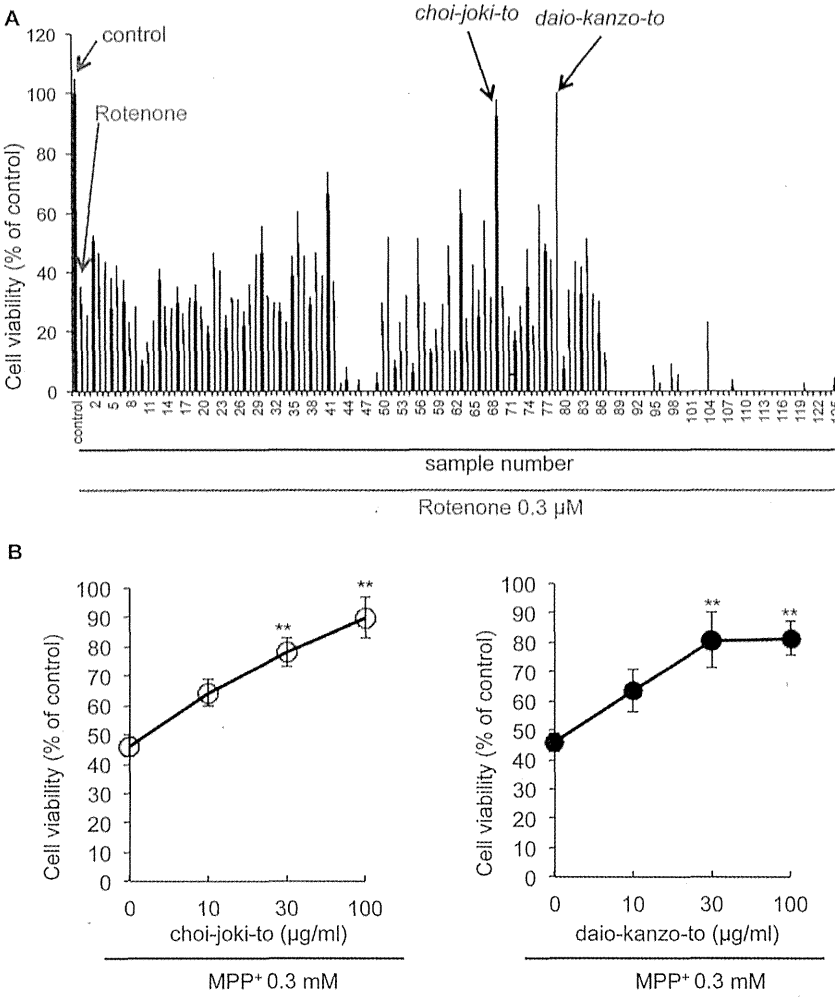

Figure 1. Two herbal medicines, *daio-kanzo-to* and *choi-joki-to*, identified as neuroprotective agents in the course of screening. (**A**) NGF-differentiated PC12D cells were treated with 0.3 μM rotenone and herbal medicine extract for 48 h. Cell viability was evaluated by trypan blue dye exclusion assay. (**B**) NGF-differentiated PC12D cells were treated with various concentrations of *choi-joki-to* or *daio-kanzo-to* in the presence of 0.3 mM MPP^+ for 48 h. Cell viability was evaluated by trypan blue dye exclusion assay. Values are the means of triplicate samples; bars, s.d. $^{**}p<0.01$ compared with MPP^+ group cells.
doi:10.1371/journal.pone.0100395.g001

insufficient [28]. Therefore, in this study, we screened a library containing 128 traditional herbal medicines, which have been used clinically for at least 10 years in Japan, focusing on their neuroprotective effects using PD-like cellular models of cell death by mitochondrial toxins, and found the anti-Parkinsonian herbal medicines *choi-joki-to* and *daio-kanzo-to*. Moreover, we identified licopyranocoumarin and glycyrurol derived from the genus *Glycyrrhiza* as common components contained in these two herbal medicines, and found they exerted neuroprotective effects against MPP^+-induced toxicity.

Results

Identification of *choi-joki-to* and *daio-kanzo-to* as potent neuroprotective herbal medicines using *in vitro* PD-like model screening

Rotenone, a direct inhibitor of mitochondria complex I, is usually employed to mimic Parkinsonism *in vitro* and *in vivo* [29]. Treatment of NGF-differentiated PC12D cells [30] with 0.3 μM of rotenone for 48 h caused marked cell death as evaluated by the trypan blue dye exclusion assay. Using this PD-like model, we screened a library containing 128 traditional herbal medicines, which have been used clinically in Japan, focusing on preventive effects against rotenone-induced cell death of NGF-differentiated PC12D cells.

As a result, several ethyl acetate (EtOAc) extracts of herbal medicines showed suppressive effects against rotenone-induced cell death generally, but two traditional herbal medicines, *choi-joki-to* and *daio-kanzo-to* exerted significant neuroprotective effects against rotenone-induced neurotoxicity (Figure 1A). Furthermore, the EtOAc extracts of *choi-joki-to* or *daio-kanzo-to* also conferred dose-dependent protection from neuronal cell death induced by MPP^+, another well-known PD-like cellular model (Figure 1B).

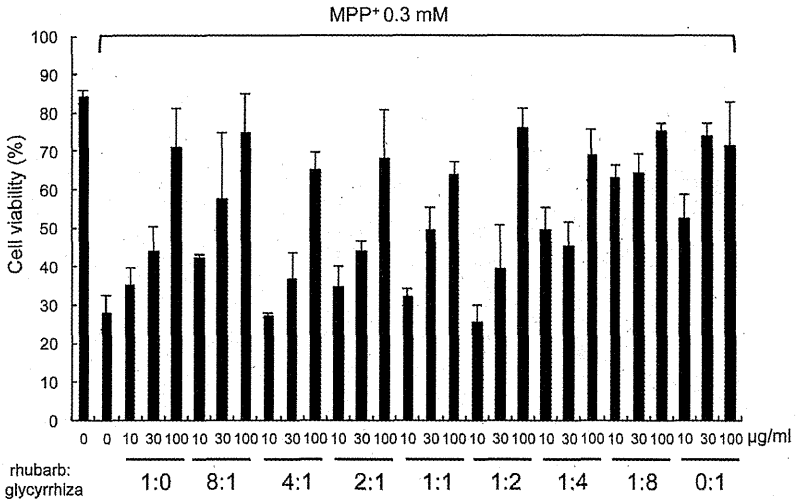

Figure 2. *Glycyrrhiza* prevented MPP$^+$-induced cell death more potently than rhubarb. NGF-differentiated PC12D cells were treated with various concentrations of rhubarb and *Glycyrrhiza* (rhubarb:*Glycyrrhiza* ratio = 1:0, 8:1, 4:1, 2:1, 1:1, 1:2, 1:4, 1:8, 0:1) in the presence of 0.3 mM MPP$^+$ for 48 h. Cell viability was evaluated by trypan blue exclusion assay. Values are the means of three independent experiments; bars, s.d. $^{**}p<0.01$ compared with MPP$^+$ group cells.
doi:10.1371/journal.pone.0100395.g002

Licopyranocoumarin and glycyrurol isolated from *Glycyrrhiza* as potent neuroprotective compounds

Next, we attempted to identify the major components responsible for neuroprotective effects contained in *choi-joki-to* and *daio-kanzo-to*. First, we noted that both *choi-joki-to* and *daio-kanzo-to* commonly contain rhubarb and *Glycyrrhiza* species, at the ratio of 2:1 (Table 1). Therefore, we examined whether this 2:1 ratio of rhubarb to *Glycyrrhiza* is important for neuroprotective effects against MPP$^+$-induced toxicity. As shown in Figure 2, rhubarb and *Glycyrrhiza* contained in *choi-joki-to* and *daio-kanzo-to* at 2:1 is not a special ratio necessary for neuroprotective effects, but rather increased *Glycyrrhiza* content potentiated the neuroprotective activity against MPP$^+$-induced cell death. Thus, we attempted to isolate the active principle responsible for neuroprotective effects from EtOAc extract of *Glycyrrhiza* by monitoring the inhibitory activity of MPP$^+$-induced NGF-differentiated PC12D cell death using a trypan blue dye exclusion assay. As a result, we isolated 10.8 mg of licopyranocoumarin (LPC) and 4.0 mg of glycyrurol (GCR) from 50 g of *Glycyrrhiza* powder as potent neuroprotective compounds (Figure 3A, B). Both LPC and GCR markedly blocked MPP$^+$-induced cell death in a dose-dependent manner with IC_{50} values of 0.9 μM and 1.2 μM, respectively (Figure 3C). Furthermore, both LPC and GCR did not show cytoprotective effects against other toxins, such as taxol and cisplatin (CDDP) even at 3 μM concentration, which significantly suppressed MPP$^+$-induced cell death in PC12D cells. Therefore, cytoprotective ability of LPC and GCR may specific for mitochondrial toxins (Figure 3D). To further verify the inhibitory effect of LPC and GCR on MPP$^+$-induced cell death, PC12D cells were labeled with PI and histogram analysis-related nuclear DNA contents were ascertained by flow cytometry. By the treatment of PC12D cells with 0.3 mM of MPP$^+$, NGF-differentiated PC12D cells with DNA content below G1 phase levels (defined as hypodiploid sub-G1 peak) were distinguishable in the population as compared with control levels (49.63±6.41% versus 7.23±1.04% of cells in sub-G1, respectively) (Figure 4A,B). LPC or GCR alone did not show any effects on the overall population of cells. However, they decreased the percentage of MPP$^+$-induced cell death by 11.2–29.0% and 11.4–28.0% (values are the mean of average of three data), respectively (Figure 4A,B), confirming that LPC and GCR inhibited MPP$^+$-induced cell death.

Licopyranocoumarin and glycyrurol attenuate the MPP$^+$-induced decrease in mitochondrial membrane potential

MPP$^+$ is a well-known inhibitor of mitochondria complex I and induces mitochondrial dysfunction. Because LPC or GCR suppressed MPP$^+$-induced cell death, we next surveyed the effect of LPC and GCR on MPP$^+$-mediated loss of mitochondrial membrane potential ($\Delta\Psi_{mit}$) using JC-1 dyes. As shown in Figure 5, by the treatment of PC12D cells with 0.3 mM of MPP$^+$ for 48 h, $\Delta\Psi_{mit}$ was decreased to 45–50% as estimated from decrease of JC-1 aggregate fluorescence. LPC or GCR alone did not affect $\Delta\Psi_{mit}$. Compared with the group treated with MPP$^+$ alone, fluorescent intensities increased in a dose-dependent manner following addition of LPC and GCR individually, indicating that LPC and GCR each inhibited MPP$^+$-induced decrease of $\Delta\Psi_{mit}$.

Licopyranocoumarin and glycyrurol counteract MPP$^+$-induced ROS production

MPP$^+$ has been extensively reported to evoke generation of reactive oxygen species (ROS). Figure 6 showed cytofluorometric histograms of NGF-differentiated PC12D cells after 12 h of treatment with 0.3 mM MPP$^+$ upon staining with CMH_2DCFDA. ROS levels were significantly increased from 100±7.8% (control level) to 247±14.9% ($p<0.001$). However, the generation of intracellular ROS was reduced to 164±15.7% ($p<0.01$) and 153±13.0% ($p<0.01$) by the addition of 3 μM LPC and 3 μM GCR, respectively.

Antioxidant activities of licopyranocoumarin and glycyrurol *in vitro*

Because treatment of PC12D cells with LPC and GCR each effectively reduced MPP$^+$-induced ROS generation, the free radical scavenging activities of these two compounds were

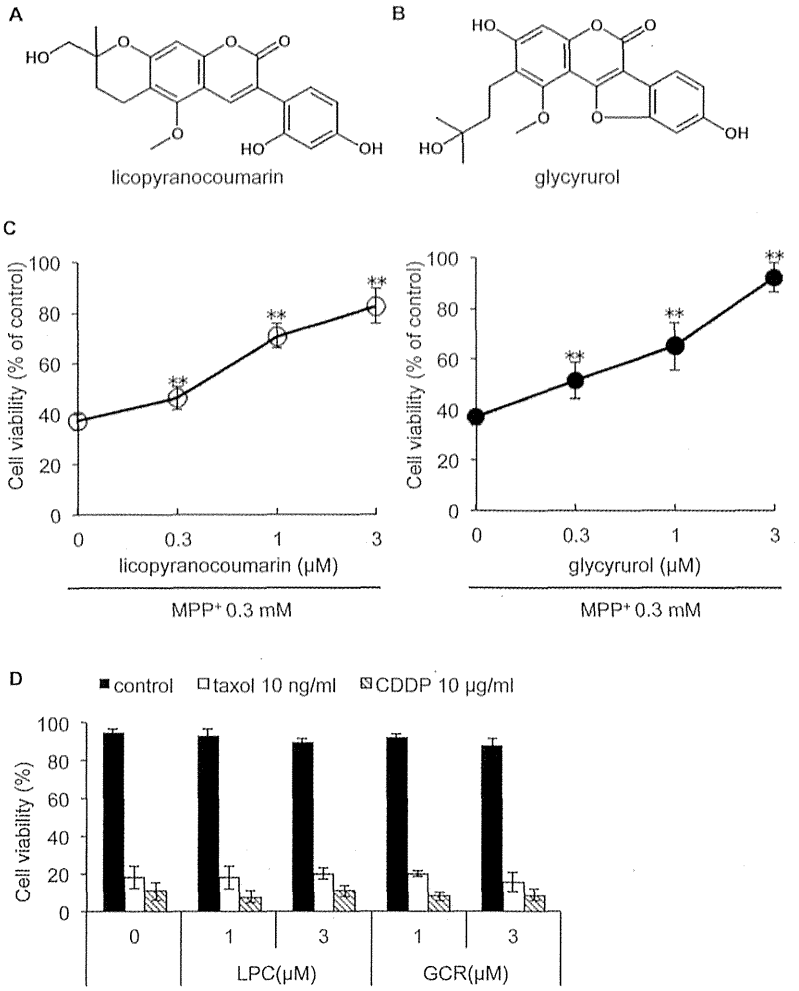

Figure 3. Licopyranocoumarin and glycyrurol prevented MPP^+-induced cell death. Structures of (**A**) licopyranocoumarin (LPC) and (**B**) glycyrurol (GCR). (**C**) NGF-differentiated PC12D cells were treated with various concentrations of LPC or GCR in the presence of 0.3 mM MPP^+ for 48 h. Cell viability was evaluated by trypan blue dye exclusion assay. (**D**) PC12D cells were treated with various concentration of LPC or GCR in the presence of 10 ng/ml taxol or 10 μg/ml cisplatin (CDDP) for 48 h. Values are the means of three independent experiments; bars, s.d. $^{**}p<0.01$ compared with MPP^+ group cells.
doi:10.1371/journal.pone.0100395.g003

examined. When the antioxidant activity of LPC and GCR were evaluated by β-carotene bleaching assay, LPC and GCR inhibited less than 10% of the carotene bleaching even at the final concentration of 30 μM (Figure 7A). The DPPH free radical scavenging potentials of LPC and GCR at 30 μM each showed little to no scavenging activity (Figure 7B). These results indicated that LPC and GCR did not possess antioxidant activity *in vitro*.

Licopyranocoumarin and glycyrurol attenuate JNK activity induced by MPP^+

It is well-established that JNK plays a central role in the mediation of MPP^+-induced neurotoxicity [31,32,33,34]. Particularly, MPP^+-induced ROS generation is reported to be closely associated with JNK activation [35]. Thus, we investigated whether the ability of LPC or GCR to reduce MPP^+-induced cell death involves the alteration of JNK signaling in MPP^+-induced neurotoxicity. As shown in Figure 8A, phosphorylated JNK levels were increased after exposure to MPP^+ for 36 h, and treatment with LPC or GCR significantly reduced the expression levels of the phosphorylated protein. In addition, a JNK inhibitor, SP600125, led to attenuation of the MPP^+-induced neuronal cell death and decreased $\Delta\Psi_{mit}$ (Figure 8B, C). These results suggest that MPP^+-induced lowering of $\Delta\Psi_{mit}$, which leads to neuronal cell death, were mediated by JNK, and neuroprotective activity of LPC and GCR against MPP^+-induced neuronal cell death might be due to downregulation of ROS generation, resulting in the inhibition of JNK activation.

Discussion

Both *choi-joki-to* and *daio-kanzo-to* are traditional herbal medicines available in Japan (called *kanpo* in Japan in particular) that are usually used for laxative products. In the laboratory, *choi-joki-to* exhibited oxygen radical scavenging capacity [36] and inhibited the progression of atheroma in a KHC rabbit model [37], On the other hand, *daio-kanzo-to* has provided inhibition of amylase

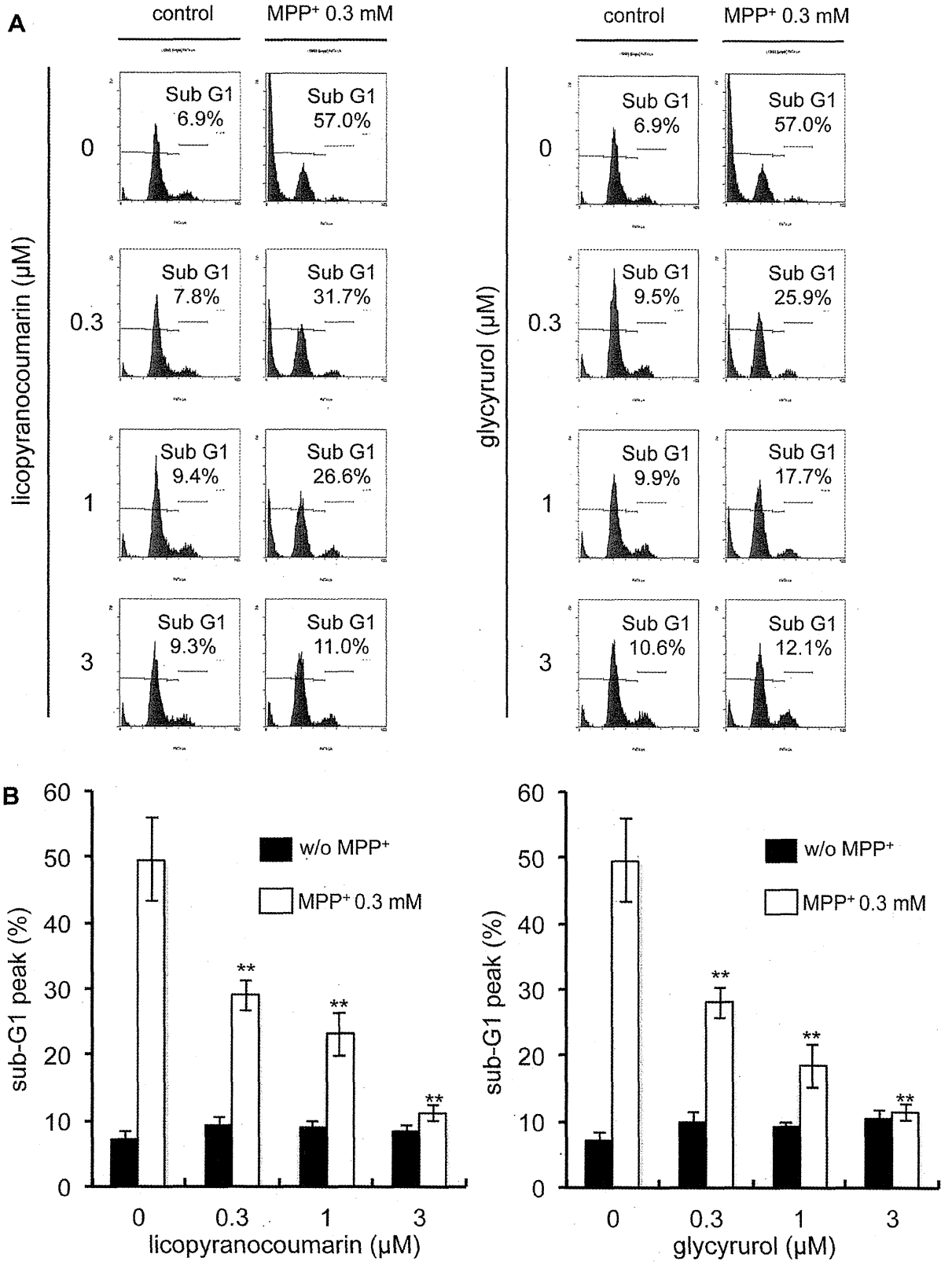
A
control
MPP+ 0.3 mM
licopyranocoumarin (μM)
glycyrurol (μM)
0
0.3
1
3
Sub G1 6.9%
Sub G1 57.0%
Sub G1 7.8%
Sub G1 31.7%
Sub G1 9.4%
Sub G1 26.6%
Sub G1 9.3%
Sub G1 11.0%
Sub G1 6.9%
Sub G1 57.0%
Sub G1 9.5%
Sub G1 25.9%
Sub G1 9.9%
Sub G1 17.7%
Sub G1 10.6%
Sub G1 12.1%
B
sub-G1 peak (%)
w/o MPP+
MPP+ 0.3 mM
licopyranocoumarin (μM)
glycyrurol (μM)
**

Figure 4. Licopyranocoumarin and glycyrurol attenuated MPP^+-induced apoptosis. (**A**) NGF-differentiated PC12D cells were treated with various concentrations of licopyranocoumarin or glycyrurol in the presence of 0.3 mM MPP^+ for 48 h. Collected cells were stained with PI and analyzed by flow cytometry. (**B**) The sub G1 ratio was analyzed. Values are the means of three independent experiments; bars, s.d. $^{**}p<0.01$ compared with MPP^+ group cells.
doi:10.1371/journal.pone.0100395.g004

activity in mouse plasma and gastrointestinal tube [38], inhibition of cholera toxin [39], and inhibitory effects on drug oxidations [40]. In this study, we have demonstrated that *choi-joki-to* and *daio-kanzo-to* had neuroprotective effects against MPP^+- and rotenone-induced toxicity in NGF-differentiated neuronal PC12D cells. Furthermore, we identified that *Glycyrrhiza*, commonly contained in these two herbal medicines, possessed potent neuroprotective activity against MPP^+-induced toxicity. *Glycyrrhiza* is contained in a number of traditional herbal medicines including *yi-gan san* previously identified as neuroprotective agents against mitochondrial toxins, therefore, we investigated relationships between the neuroprotective effects of traditional herbal medicines and their contents of *Glycyrrhiza*. The correlation coefficient between neuroprotective effects of traditional herbal medicines and contents of *Glycyrrhiza* in each herbal medicine was calculated at 0.20 (Figure S1), indicating a very weak relationship. This weak relationship might be explained by our finding that higher concentration of *Glycyrrhiza* (300 μg/ml) showed cytotoxic effect in PC12D cells (Figure S2). Another possible explanation is that other constituent of traditional herbal medicines, such as rhubarb, also exerted neuroprotective effects in PC12D cells (Figure 2). Major components of *Glycyrrhiza* are triterpenoid saponins, and glycyrrhizin and its metabolite. These compounds show several potential health effects including anti-inflammatory, anti-viral, hepatoprotective, anti-cancer and immunomodulatory effects [41]. Therefore, at first we predicted that glycyrrhizin might be an active principle contained in *Glycyrrhiza* that suppressed MPP^+- and rotenone-induced toxicity, but glycyrrhizin did not show such activities. Instead, we isolated the coumarin derivatives, licopyranocoumarin (LPC) and glycyrurol (GCR), as the most potent neuroprotective compounds in *Glycyrrhiza*. LPC isolated from *Glycyrrhiza* sp. has been reported to show several bioactivities, including anti-HIV effects and inhibition of CYP3A4 and the aryl hydrocarbon receptor antagonist [42,43,44]. On the other hand, GCR, which was very recently isolated from *Glycyrrhiza uralensis*, shows antithrombotic effects [45]. However, so far the neuroprotective effects of these two compounds have not yet been reported. This study has indeed revealed, for the first time, the potent neuroprotective activity of LPC and GCR in a PD-like cellular model system. LPC and GCR also inhibited rotenone-induced cell death in HeLa cells; however, the effects in HeLa cells were quite weak when compared to that seen in PC12D cells (Figure S3). Therefore, LPC and GCR seem to prefer to exert cytoprotection in neuronal cells. Oxidative stress associated with a general dysfunction of mitochondrial homeostasis is a leading hypothesis as a potential mechanism for dopaminergic neuronal degeneration in PD [46]. Postmortem analyses of the substantia nigra from PD patients confirm several oxidative stress-related alterations [47,48,49], and several toxins (rotenone, paraquat, and MPP^+) used to produce PD-animal models directly and/or indirectly inhibit mitochondrial function, induce the production of ROS, and promote oxidative damage. Therefore, antioxidant ingredients are considered to be promising approach to prevent the disease progression. For example, α-tocopherol, coenzyme Q_{10} and catechols have been reported to exert neuroprotective effects by attenuating rotenone-induced oxidative stress on rotenone models *in vitro* and *in vivo* [50,51,52]. Likewise, we found that LPC and GCR attenuated the MPP^+-induced increase in intracellular ROS generation (Figure 6A), indicating that inhibition of MPP^+-mediated ROS generation is closely related to the neuroprotective effects of LPC and GCR. Several lines of evidence have suggested that ROS generation induces the activation of JNK signaling, and JNK represents one of the major signaling pathways implicated in PD pathogenesis. JNK activity is increased in MPTP animal models [53,54,55,56], MPP^+-treated cell culture models [35,54], and rotenone neurotoxicity [57,58]. Moreover, ROS-mediated activation of JNK almost inevitably leads to cell death. Indeed, we also confirmed that a JNK inhibitor, SP600125, suppressed MPP^+-induced cell death (Figure 8B), and MPP^+-induced activation of JNK and cell death were found to be inhibited by LPC and GCR under conditions where LPC or GCR inhibited the MPP^+-mediated ROS generation (Figure 8A). Although the potential mechanisms by which JNK participates in MPP^+-induced cell death remains to be fully determined, activation of JNK has been reported to mediate cell death by participating in the induction of mitochondrial permeability transition (mPT) and decrease of $\Delta\Psi_{mit}$ in subsets of cell types [59,60]. Because in our assay system SP600125 inhibited both cell death and the decrease in $\Delta\Psi_{mit}$ induced by MPP^+ (Figure. 8B and C), we consider the inhibition of the decrease in MPP^+-induced $\Delta\Psi_{mit}$ caused by LPC and GCR (Figure 5) to be due to the inhibition of ROS-mediated JNK activation.

Several neuroprotective compounds have significant antioxidant and free radical-scavenging activities. LPC and GCR are members of the coumarin compound family. There have been several reports on the antioxidant activities of coumarins [61,62,63], and LPC and GCR each inhibited MPP^+-induced ROS generation. Nevertheless, neither LPC nor GCR possessed ROS scavenging activity *in vitro*. Increased amount of ROS can be generated by an imbalance of antioxidant enzymes and activation of the oxidase

Table 1. Crude drugs constituents of "*choi-joki-to*" and "*daio-kanzo-to*".

choi-joki-to		*daio-kanzo-to*	
Scientific names	**Contents (g)**	**Scientific names**	**Contents (g)**
rhubarb	2	rhubarb	4
glycyrrhiza	1	*glycyrrhiza*	2
Salt cake	0.5		

doi:10.1371/journal.pone.0100395.t001

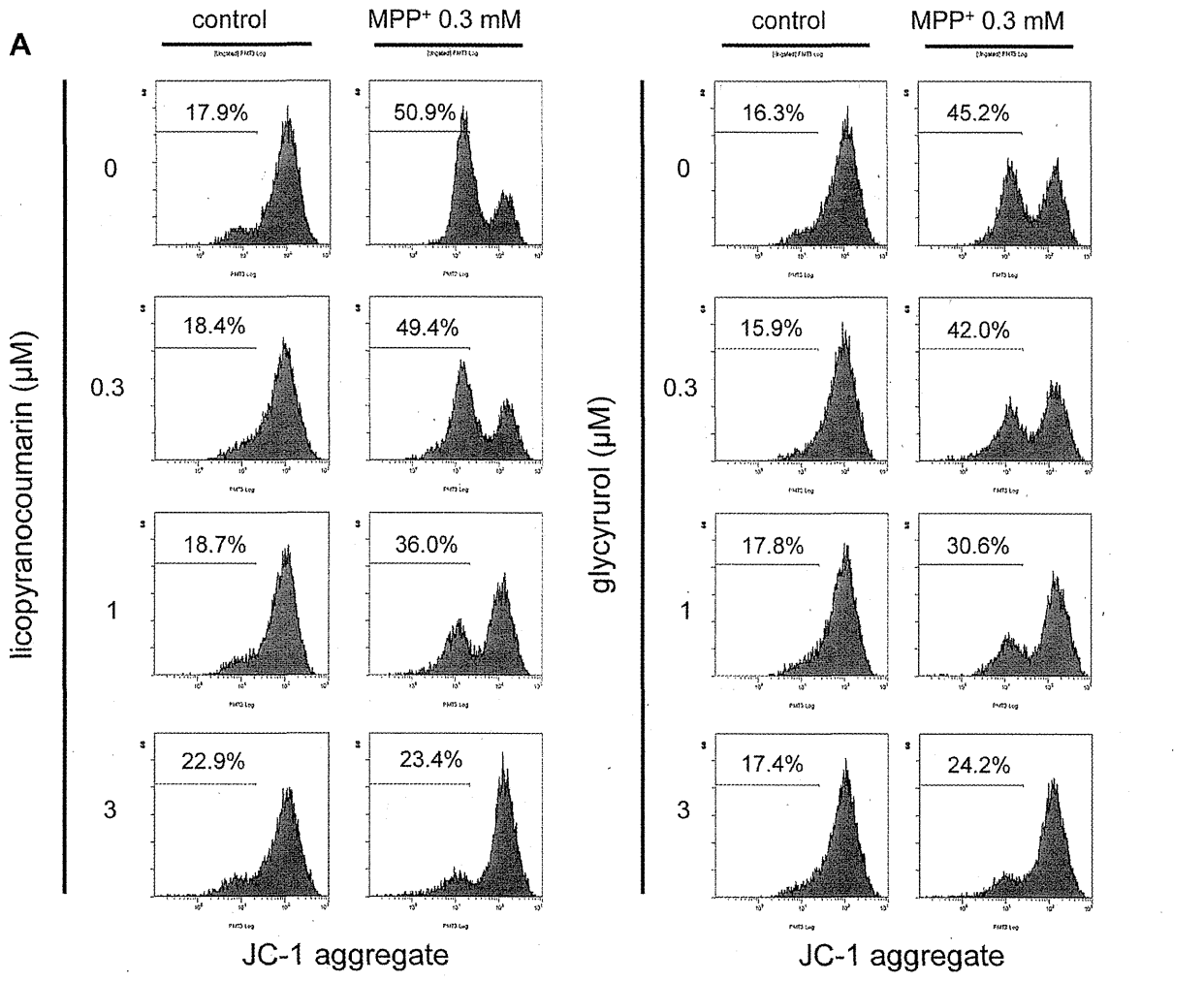
A
control
MPP+ 0.3 mM
control
MPP+ 0.3 mM
licopyranocoumarin (μM)
glycyrurol (μM)
0
0.3
1
3
17.9%
50.9%
18.4%
49.4%
18.7%
36.0%
22.9%
23.4%
16.3%
45.2%
15.9%
42.0%
17.8%
30.6%
17.4%
24.2%
JC-1 aggregate
JC-1 aggregate

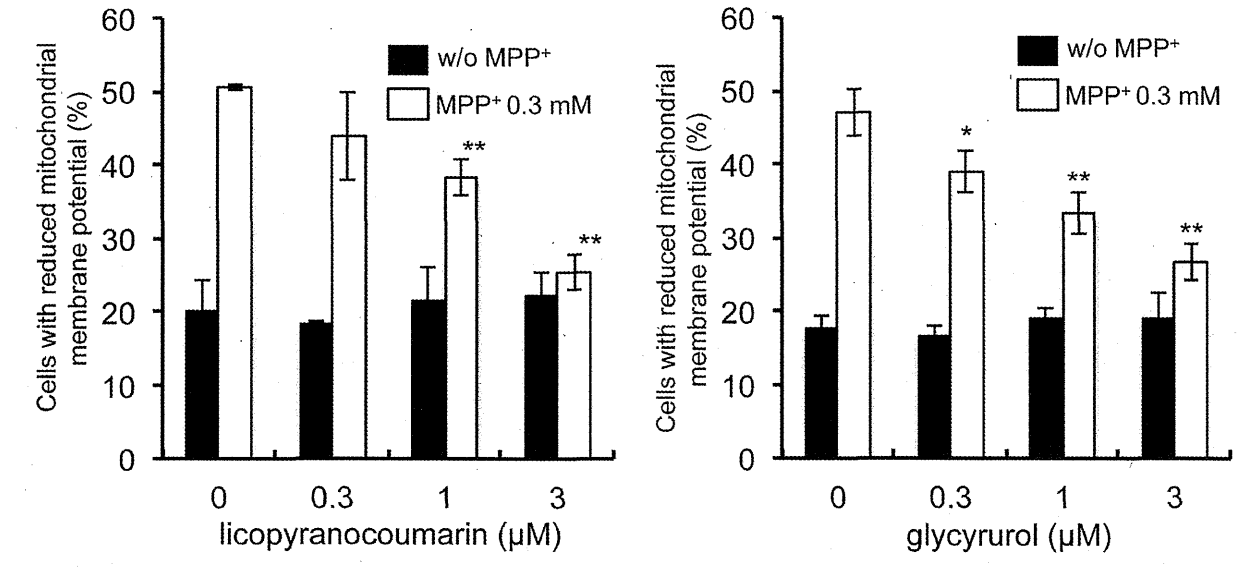
B
Cells with reduced mitochondrial membrane potential (%)
w/o MPP+
MPP+ 0.3 mM
licopyranocoumarin (μM)
glycyrurol (μM)
0
0.3
1
3
10
20
30
40
50
60
*
**